

ANALYZING MICROWAVE SPECTRA COLLECTED BY  
THE SOLAR RADIO BURST LOCATOR

Cheryl-Annette Kincaid, B.A.

Thesis Prepared for the Degree of  
MASTER OF SCIENCE

UNIVERSITY OF NORTH TEXAS

May 2007

APPROVED:

Armin R. Mikler, Major Professor  
Yan Huang, Committee Member  
Rada F. Mihalcea, Committee Member  
Joel B. Mozer, Committee Member  
Krishna Kavi, Chair of the Department of  
Computer Science and Engineering  
Oscar Garcia, Dean of the College of  
Engineering  
Sandra L. Terrell, Dean of the Robert B.  
Toulouse School of Graduate Studies

Kincaid, Cheryl-Annette, Analyzing Microwave Spectra Collected by the Solar Radio Burst Locator. Master of Science (Computer Engineering), May 2007, 76 pp., 4 tables, 33 illustrations, references, 22 titles.

Modern communication systems rely heavily upon microwave, radio, and other electromagnetic frequency bands as a means of providing wireless communication links. Although convenient, wireless communication is susceptible to electromagnetic interference. Solar activity causes both direct interference through electromagnetic radiation as well as indirect interference caused by charged particles interacting with Earth's magnetic field.

The Solar Radio Burst Locator (SRBL) is a United States Air Force radio telescope designed to detect and locate solar microwave bursts as they occur on the Sun. By analyzing these events, the Air Force hopes to gain a better understanding of the root causes of solar interference and improve interference forecasts.

This thesis presents methods of searching and analyzing events found in the previously unstudied SRBL data archive. A new Web-based application aids in the searching and visualization of the data. Comparative analysis is performed amongst data collected by SRBL and several other instruments. This thesis also analyzes events across the time, intensity, and frequency domains. These analysis methods can be used to aid in the detection and understanding of solar events so as to provide improved forecasts of solar-induced electromagnetic interference.

Copyright 2007

by

Cheryl-Annette Kincaid

## ACKNOWLEDGEMENTS

There are many people who deserve a great deal of thanks for their involvement with my education, research, and thesis endeavors. My family, friends, professors, and co-workers have been very supportive throughout the thesis process, and for this I am very grateful.

Specifically, I would like to thank each of my committee members for their involvement and feedback. Drs. Yan Huang and Rada Mihalcea graciously agreed to serve on my committee providing valuable feedback. Dr. Armin Mikler spent many hours reviewing my research and offering guidance. Dr. Joel Mozer served as both my mentor during my summer research for the Air Force Research Laboratory as well as a member of my thesis committee. His knowledge and enthusiasm helped to inspire me to pursue a research topic that would combine both computing and solar physics.

I would also like to thank the people who have spent numerous hours reading over portions of my thesis providing comments, questions, and edits. A very grateful thank you in this area is given to Cary Spratt and to my dad.

Finally, I would like to thank my dear friend and fiancé, Brandon Parker, for his patience and persistence throughout the thesis process. Time and again he has gone well beyond the call of duty in finding ways to help. Whether it was helping to locate a hard to find reference, editing, fighting laser printers, or even fading into the background, he was willing to help in whatever way was most needed at the time. Thank you, Brandon, for all you've done to encourage me to reach my goals.

## NOTE

During the time that this thesis was being written, the Air Force changed the names of both the Solar Radio Burst Locator (SRBL) and the Improved Solar Observing Optical Network (ISOON). SRBL is now known as the Radio Solar Patrol Network (RSPaN), and ISOON now bears the name of the Optical Solar Patrol Network (OSPaN). This thesis refers to these instruments by their previous nomenclature.

# CONTENTS

	Page
ACKNOWLEDGEMENTS .....	iii
NOTE .....	iv
LIST OF TABLES .....	viii
LIST OF FIGURES.....	ix
Chapter	
1. INTRODUCTION .....	1
1.1 Overview .....	1
1.2 The Sun .....	2
1.3 Earth .....	5
1.4 The Sun-Earth Connection.....	7
2. SOLAR RADIO BURST LOCATOR.....	13
2.1 Overview .....	13
2.2 History .....	14
2.3 Design.....	15
2.3.1 Outdoor Hardware .....	16
2.3.2 Indoor Hardware .....	18
2.3.3 Software .....	19
2.4 Existing Functionality .....	20
2.5 Goals for SRBL .....	22
3. ANALYSIS METHODOLOGIES.....	27
3.1 Purpose of Analysis .....	27
3.2 Method of Collection and Format of Data.....	28
3.3 Analysis Methodologies Overview.....	28
3.3.1 Manual Analysis.....	29
3.3.2 Hybrid Method - Programmatic and Manual Analysis ....	30
3.3.3 Automated Method (Tool Development & Event Searchability) .....	35

3.4	Tool Development .....	36
3.4.1	Parameter Selection .....	37
3.4.2	Search Results .....	39
3.4.3	Summary Data.....	40
4.	ANALYSIS RESULTS.....	41
4.1	Comparative Analysis of Instrumentation.....	41
4.1.1	Timings .....	43
4.1.2	Intensity Comparisons .....	43
4.2	Brightening Classification Analysis.....	45
4.2.1	Blips.....	45
4.2.2	Early Morning.....	46
4.2.3	End of Day .....	47
4.2.4	Human Induced .....	48
4.2.5	Long.....	49
4.2.6	Probable Burst.....	50
4.2.7	Probable but Weak .....	52
4.2.8	Short .....	53
4.2.9	Undetermined .....	54
4.2.10	Classification Summary .....	54
4.3	Analytical Metrics .....	55
4.3.1	Duration Analysis.....	56
4.3.2	Burst Time vs. Intensity Analysis .....	58
4.3.3	Burst Frequency vs. Intensity Analysis .....	62
4.3.4	Temporal Analysis of Horizon Events .....	64
4.3.5	Other Findings .....	66
5.	SUMMARY AND CONCLUSION.....	69
5.1	Summary.....	69
5.2	Future Works.....	70
5.2.1	Analysis Enhancements .....	70
5.2.2	Classification Enhancements.....	70
5.2.3	Precursor Study.....	71
5.2.4	Tool Enhancement.....	71

5.2.5	Incorporating Location Information .....	72
5.3	Conclusion .....	72
REFERENCES	.....	73



## LIST OF TABLES

	Page
3.1 SRBL frequency ranges .....	32
3.2 Frequency subgroup color legend .....	32
3.3 Event criteria.....	36
4.1 Number of events that corresponded with SRBL readings in various wavebands .....	42

## LIST OF FIGURES

	Page
1-1 Sun components.....	3
1-2 Solar wind and the Earth's magnetosphere .....	6
2-1 SRBL design schematics.....	16
2-2 SRBL antennas .....	17
2-3 SRBL log-spiral antenna.....	18
2-4 SRBL indoor hardware .....	19
3-1 An event image.....	33
3-2 SRBL online data analyzer .....	39
4-1 Graphical comparison of SRBL vs GEOS-12 readings.....	44
4-2 Blip - June 24, 2004 - Duration: 0 hr, 0 minutes, 30 seconds .....	46
4-3 Early Morning - July 23, 2004 - Duration: 1 hr, 19 minutes, 18 seconds .....	47
4-4 End of Day - July 11, 2004 - Duration: 0 hr, 8 minutes, 2 seconds.....	47
4-5 Human Induced - July 13, 2004 - Duration: 0 hr, 6 minutes, 33 seconds .....	48
4-6 Long - July 30, 2004 - Duration: 2 hr, 1 minute, 44 seconds .....	49
4-7 Long - February 1, 2005 - Duration: 1 hr, 12 minutes, 35 seconds.....	49
4-8 Long - March 7, 2005 - Duration: 1 hr, 23 minutes, 4 seconds .....	50
4-9 Probable Burst - July 23, 2004 - Duration: 0 hr, 10 minutes, 38 seconds.....	51
4-10 Misclassified as Probable Burst - August 8, 2004 - Duration: 42 minutes, 46 seconds .....	51
4-11 Probable but Weak - July 18, 2004 - Duration: 0 hr, 7 minutes, 22 seconds ....	52
4-12 Short - July 14, 2005 - Duration: 0 hr, 1 minute, 58 seconds.....	53
4-13 Undetermined - April 29, 2005 - Duration: 0 hr, 27 minutes, 12 seconds .....	54
4-14 Solar event durations.....	56

4-15	Short burst with long tail November 8, 2004 - Total duration: 0 hours, 45 minutes, 13 seconds .....	57
4-16	Long burst with multiple peaks November 9, 2004 - Duration: 0 hours, 56 minutes, 31 seconds.....	58
4-17	Intensity curve .....	59
4-18	July 23, 2004 - Intensity comparison .....	60
4-19	Average intensity over time .....	61
4-20	Average intensity over time .....	62
4-21	Frequency intensities.....	63
4-22	Early Morning brightening temporal analysis.....	64
4-23	End of Day temporal analysis.....	65
4-24	July 7, 2005 - Duration: 0 hours, 38 minutes, 1 second.....	66
4-25	SRBL burst locations for simultaneous events .....	68

## CHAPTER 1

### INTRODUCTION

#### 1.1 Overview

Modern communication systems rely heavily upon microwave, radio, and other electromagnetic frequency bands as a means of providing wireless communication links. Over the past century wireless communication has greatly expanded.

Although convenient, wireless communication is quite susceptible to electromagnetic interference. A major source of this interference is the Sun. Solar activity causes both immediate interference through electromagnetic radiation as well as delayed interference caused by charged particles interacting with Earth's magnetic field.

Additionally, solar-induced geomagnetic storms have been known to cause power outages, radiation dangers for astronauts, and disturbances in land-based communication systems.

One group that is interested in predicting solar storms that cause these problems is the United States Air Force. To this end, the Air Force has established several programs to study space weather, provide event reports, and research means of improving forecasts. One of the instruments designed to aid in these goals is the Solar Radio Burst Locator (SRBL). This thesis focuses on analyzing data collected by SRBL over the past several years.

The remaining portion of this chapter provides background information on space weather and its effects. Section 1.2 describes the Sun and several of the mechanisms

that contribute to solar storms. Section 1.3 provides a description of Earth's defenses to space weather, and Section 1.4 introduces problems caused by the interaction of space weather and the earth.

## 1.2 The Sun

The Sun is the driving force of space weather in the Solar System, producing flares, coronal mass ejections (CMEs), and the solar wind. It is also the most powerful electromagnetic transmitter in the Solar System, producing wavelengths spanning from low frequency radio bands to high frequency x-rays.

Chemically, the Sun consists primarily of hydrogen. Approximately 91.2% of its atomic composition, or 71.0% of its mass, is of this element. Helium is the second most abundant element, and together hydrogen and helium comprise approximately 99.9% of the Sun's atomic composition, or 98.1% of its mass [4] [18].

Hydrogen, consisting of a single proton and electron, is a relatively unstable element. Electrons are easily stripped, leaving charged particles. This plasma is highly conductive and very responsive to the influence of magnetic fields.

As depicted in Figure 1-1, the Sun has several distinct layers. These layers are the core, the radiation zone, the convection zone, the photosphere, the chromosphere, the corona, and the heliosphere.

The core is extremely dense and is the center of nuclear fusion reactions that combine hydrogen into heavier elements and produce heat and photons. The core's average temperature is nearly 15,000,000 K. This heat is transferred outward first by

radiation and then by thermal convection. At the photosphere, the visible surface of the Sun, the temperature is approximately 6,000 K.

Beyond the photosphere are several layers of the Sun's atmosphere. These include the chromosphere, the corona, and the heliosphere. The chromosphere extends for approximately 2,000 km, and the temperature in this region slowly increases with altitude up to 100,000 K. Beyond the chromosphere is a sparse but very hot region of the Sun known as the corona where temperatures rise to nearly 1,000,000 K before they drop again further away from the Sun. The heliosphere is the outermost region of the Sun's atmosphere, and it continues to the edges of the solar system.

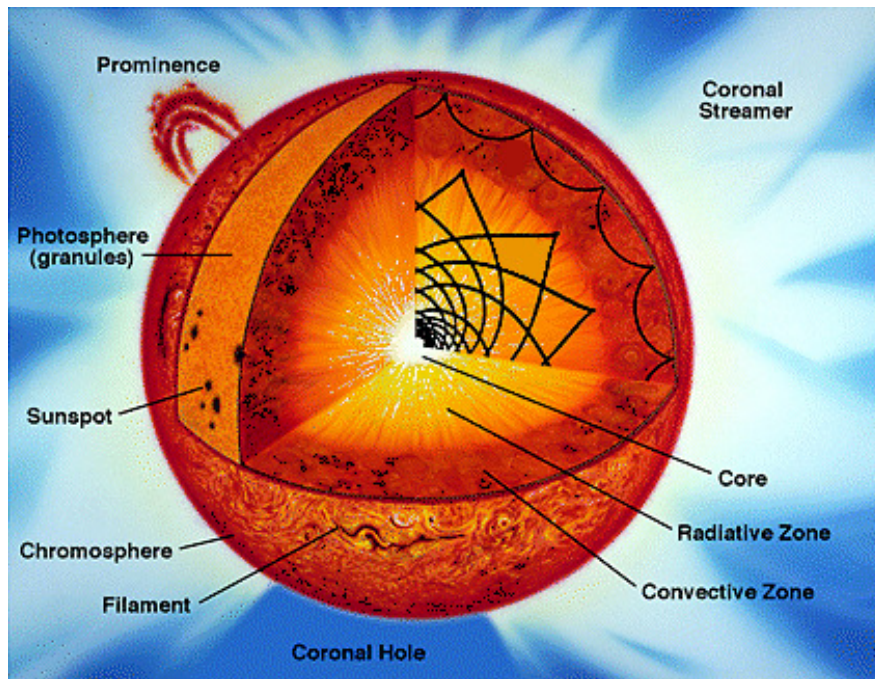


Figure 1-1 Sun components.  
Courtesy NASA/JPL-Caltech.

Since the Sun is not solid, its rotational velocity is not uniform. Thus, for a full rotation, the Sun takes about twenty-five days at the equatorial latitudes and about thirty-five days at the polar regions [14]. This differential rotation adds to the Sun's already complex electric and magnetic characteristics. As the Sun rotates, magnetic fields become stretched, pulled, and twisted. Over time, they begin to interconnect and form regions of increased activity including sunspots, flares, and violent solar eruptions.

Approximately every 11.1 years, the Sun goes through a cycle of high and low activity. This activity is governed by the Sun's complex magnetic field and its twisting from the Sun's differential rotation. As the Sun becomes more active and approaches solar maximum, the number of sunspots, flares, and other visible events increase. With this increased activity comes an increase in the events that cause geomagnetic storms on Earth.

One of the most obvious visual signs of the Sun's current phase in the solar cycle is the number of sunspots appearing on the Sun's photosphere. The intense magnetic fields of sunspots are believed to reduce localized convective action of the Sun, thus reducing temperatures from 6000 K to 4000 K causing sunspots to appear as dark regions. Due to their strong magnetic fields, sunspots tend to be the primary regions of solar storm activity, but active regions can form where sunspots are not evident.

Sunspots usually occur in pairs with opposite polarity. Strong magnetic fields interconnect sunspot groups, and when these fields become highly twisted, an explosive release of energy may result. These solar flares release radiation throughout the electromagnetic spectrum.

A coronal mass ejection (CME) is a powerful eruption of solar matter into interplanetary space. When a CME reaches earth, its charged particles and their associated magnetic field can interact with Earth's magnetic field causing numerous effects.

### 1.3 Earth

Earth is protected from the harsh environment of space by several mechanisms. Two of these are Earth's magnetosphere, which helps to deflect most charged particles, and Earth's ionosphere, which absorbs large amounts of harmful radiation.

The magnetosphere is Earth's magnetic field. It extends far beyond Earth's atmosphere and is shaped by the solar wind and Earth's core. Near the surface of the Earth, the magnetosphere can be thought of as a magnetic dipole. Further away from the surface, the solar wind compresses the sunward side of the field, and elongates the field in the anti-sun direction. This is depicted in Figure 1-2.



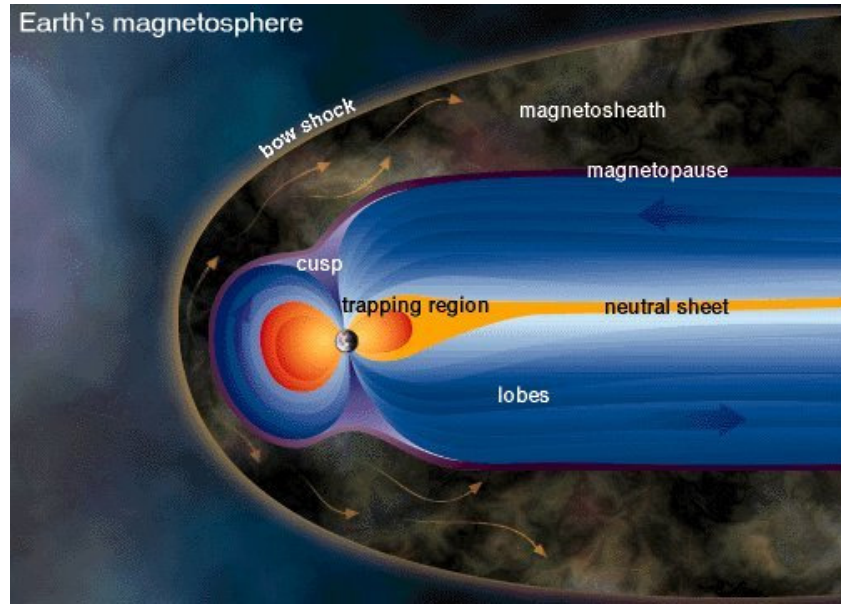


Figure 1-2 Solar wind and the Earth's magnetosphere.  
Courtesy Marshall Space Flight Center / Science@NASA.

As high speed charged particles stream from the Sun toward Earth, they encounter the bow shock region of the magnetosphere. Particles are slowed and rerouted by this force, and most are deflected around Earth entirely. However, some are not, and these particles interact with Earth's magnetic field causing numerous geomagnetic effects.

When a CME speeds toward Earth, a large number of particles (and their associated magnetic field) bombard Earth's magnetic field. When this happens, a geomagnetic storm may occur. The most well known result of this type of interaction is the production of the aurora borealis and the aurora australis, commonly known as the northern and southern lights. However, a number of other effects result that are much more harmful to our communication and energy infrastructure systems.

The second protective mechanism mentioned earlier is Earth's ionosphere. The ionosphere is the outermost region of Earth's atmosphere. It extends from about 50 km to about 500 km above Earth's surface [6]. The ionosphere is formed by solar radiation stripping electrons from atoms in the air, thus ionizing them. In the process, UV radiation is absorbed.

In addition to absorbing high energy radiation, the ionosphere is reflective to certain electromagnetic frequencies. This property is useful for long distance radio communication. Different frequencies are able to bounce off various layers of the ionosphere back to ground stations elsewhere on the planet.

#### 1.4 The Sun-Earth Connection

During solar maximum, there is an increase in Extreme Ultraviolet (EUV) radiation emanating from the sun. This results in more atmospheric atoms being stripped of electrons and becoming ionized. The increase in the ionospheric density in turn enhances the ability of the ionosphere to reflect signals back to earth. In these cases, an increase in solar activity helps communication systems.

However, this same activity can cause problems as well. During geomagnetic storms, large quantities of charged particles flow through the ionosphere creating disturbances. This can cause alternate enhancement and degradation of the reflective ability of various layers in the ionosphere. At times, multiple paths may exist for communication signals, and this may lead to an increase in interference from various broadcasters.

Additionally, geomagnetic storms can cause heating and expansion of the ionosphere. Such expansion increases the drag on satellites, slowing their orbits [3]. Eventually, the cumulative effect of this slowing results in the early return of these satellites to earth.

The charged particles themselves have also been known to cause problems for satellites [3] [17]. The electrical noise of these particles has caused bit errors in both data and in the software controlling the satellites. In some cases, these errors are correctable. Another hardware problem caused by CMEs is induced electromagnetic currents. These have been known to short out electronic components in satellites rendering them permanently useless.

Similarly induced currents have been known to happen in earth-based communication lines. One of the first times this effect was observed was in 1859 in the Boston area. During a time of strong auroral displays, telegraph lines began operating intermittently. At times, they did not operate at all. At other times, induced power from the geomagnetic storm seemed to allow them to function with their power supplies disconnected. [14]

Since then, there have been multiple occasions of land-based communication systems malfunctioning due to induced currents from geomagnetic storms. Events include such things as localized loss of long distance telephone communication, and problems with communication in one direction along the transatlantic cable. [14]

Oil pipelines have also suffered from the effect of induced currents. Current in these pipelines speeds up corrosion. Cathodic protection is in place on many pipelines to reduce corrosive action caused by normal electrochemical reactions. However,

geomagnetic storms have been known to overcompensate and thus make the corrosion even worse.

On rare occasions, induced currents have been strong enough to affect power grids and in a few instances cause power blackouts. These occurrences are most likely when the magnetic field of a CME is very strong and is oriented with its polarity in the opposite direction to the polarity of Earth's magnetic field. In 1972, a 230-kilovolt power transformer in British Columbia was burned out in this manner, and in 1989 a geomagnetic storm caused a large-scale power blackout in Quebec and the northeastern United States.

CMEs also cause an increase in harmful radiation near Earth. This can pose a danger to astronauts performing space walks [3].

In addition to the problems caused by coronal mass ejections, the Sun can cause more immediate types of communication interference as well. Some of this is predictable, and some is not known until it happens.

One predictable type of interference is a sun outage. This type of interference affects communication with geostationary satellites in the fall and the spring. As Earth approaches the time of the equinoxes, these satellites have periods of time when they are aligned directly between the Sun and the ground station trying to receive their signal. With the Sun directly behind it, the signal the satellite is sending is often lost amongst the electromagnetic noise coming from the Sun. The outages are predictable and only last for a few minutes, but currently there is nothing that can be done to prevent these outages.

A similar problem happens with other communication equipment that points in the direction of the Sun. The line of sight paths of non-geostationary satellites also pass in front of the Sun. The problems are much the same as discussed previously with geostationary satellites. The main difference is that these events can happen at any point in the year and that the duration of the interference varies depending upon the orbital path and the location of the ground station.

These types of problems are greatly compounded during times of high solar activity. Solar flares, the eruption of CMEs, and various other events on the Sun are often accompanied by intense electromagnetic bursts throughout the frequency spectrum. Emissions include low-frequency radio, mid-frequency visual, and high-frequency ultraviolet and x-ray waves. Many of these electromagnetic bursts cause direct and immediate interference to our communication systems.

Burst characteristics can be used to identify the type of solar event in progress. For example, during the eruption of a CME, plasma progresses through the various layers of the Sun's atmosphere often causing plasma oscillations and generating radio waves. The frequency of the oscillations varies at different heights in the solar atmosphere with the highest frequencies being near the solar surface, and lower frequencies occurring in the higher layers [19]. Thus, as a CME travels outward, the radio frequencies that are emitted by the expansion tend to drift from high to low. This characteristic drift is known as a Type II radio burst [14] [5]. Detecting and identifying Type II radio bursts can be one of the first indicators that a CME has occurred.

The speed at which CMEs travel away from the Sun varies between 50 km/s and 1815 km/s [14]. CMEs' travel time to Earth is generally anywhere between 18 hrs and 4

days [2]. Since electromagnetic radiation travels at the speed of light, radio bursts can help to inform us of a CME well before it reaches earth. Precautionary measures, such as temporarily turning off satellites and not scheduling space walks, can thus be taken to deal with the effects of a CME before it arrives.

Solar bursts cause communication problems when the energy they emit overpowers the reception of signals in the same frequency range. This is primarily a problem for antennas that are pointed directly toward the Sun. However, receivers have several secondary and tertiary lobes of reception. Interference can happen in any of these regions.

Solar bursts have been known to disrupt many systems including satellite communication, cell phones, global positioning system (GPS) accuracy, and radar. Although it is not currently possible to remove such interference, it is important to be able to identify the source. If a user of a system knows that problems are caused by the Sun and not by system failure or intentional jamming, then the user can better respond to the situation. Alternate frequencies may be able to be used, a different path of communication may be switched to, or the decision may be made to just wait out the interference.

Researchers are working to be able to better identify when solar events happen, the underlying cause and structure of these events, the nature and characteristics of these events, and the ways that these events affect things here on Earth. Eventually, researchers hope to be able to use this information to help predict events before they happen and so provide time for protective action to be taken.

Numerous instruments have been developed to detect electromagnetic activity emanating from the Sun. These instruments have various frequency ranges, time resolutions, and physical locations, as well as various abilities and limitations. Amongst these instruments are particle and magnetic sensors, telescopes that view various frequencies in the optical range, satellites that view the Sun's x-ray emissions, long-wave radio receivers, and higher frequency radio and microwave receivers. [8]

This thesis describes a tool designed to aid in identifying and characterizing solar events recorded by the Solar Radio Burst Locator (SRBL). Chapter 2 describes the Solar Radio Burst Locator and its method of data collection. Chapter 3 explains the methodologies used in analyzing SRBL's data, and Chapter 4 provides the results of this analysis. Conclusions and suggestions for continued work are given in Chapter 5.

## CHAPTER 2

### SOLAR RADIO BURST LOCATOR

#### 2.1 Overview

Observing the Sun in the radio spectra offers several advantages not easily available in other frequencies. Unlike visible observations, radio observations are not weather dependent. Radio and microwave frequencies are not attenuated by cloud cover. Thus observations can theoretically be made in all weather conditions. Modern communication systems tend to rely on radio frequencies in the MHz through GHz spectrum. Because of this, observing the Sun in these frequencies is useful for detecting direct interference to these methods of communication.

For these reasons, in the 1990s the Solar Radio Burst Locator (SRBL) was designed and deployed by the United States Air Force Research Laboratory. SRBL was commissioned by the Air Force to be an upgrade and replacement for the Radio Solar Telescope Network (RSTN) system. [8] [9]

RSTN is an operational network of solar radio telescopes located around the world collecting continuous solar data in all weather conditions. Site locations for the RSTN network are in Palehua, HI, USA; Sagamore Hill, MA, USA; San Vito, Italy; and Learmonth, Australia [19]. Although RSTN allows for continuous monitoring of the Sun, it is limited in its frequency resolution. RSTN only collects data at eight discrete frequencies -- 245, 410, 610, 1415, 2695, 4995, 8800, and 15400 MHz. To collect this



information, RSTN utilizes three telescopes per site, each covering different frequencies.

The information that RSTN collects is used to help determine possible interference for various communication systems. However, due to the low frequency resolution, interpolation is necessary to determine if interference is likely for systems that use frequencies that are between or outside of the frequency reception boundaries used by RSTN. Since microwave bursts tend to be broad spectrum, such interpolation is considered acceptable.

In the 1990s, the Air Force decided to expand upon RSTN's capabilities and commission a set of radio telescopes that not only had a more extensive frequency resolution, but that also had the ability to locate the approximate source of bursts on the solar disk.

## 2.2 History

SRBL was proposed to the Air Force in the early 1990s by the California Institute of Technology as a novel method of providing both continuous microwave spectrographic observations and rough burst locations for solar microwave events. SRBL was to be used as an extension of the Solar Observing Optical Network (SOON) optical telescope system. Both of these systems would then be part of the Solar Electro-Optical Network (SEON). [8] [9]

In 1994, field testing began in Haleakala, Hawaii and at the Owens Valley Radio Observatory (OVRO) with two equatorial mount antennas. Research-grade prototypes

with azimuth-elevation mounts and an expanded frequency range were built and installed shortly afterwards. [8]

In 1997, Raytheon Technical Systems Corporation was selected to build the production units. In 2001, the first production unit was installed at Holloman Air Force Base in New Mexico. However, the SEON program was cancelled before all of the production units were made. Thus, the goal of a world-wide network of SRBLs and SOONs was not realized.

In fall 2003, the Holloman SRBL was moved to Sunspot, NM where it joined a recently upgraded SOON telescope known as the Improved Solar Observing Optical Network (ISOON). SRBL would be monitored and maintained by the same group that worked with the Sunspot ISOON telescope. Between that fall and the following spring, SRBL was set up and installed. Data collection began in March 2004.

### 2.3 Design

Figure 2-1 shows a basic diagram of the various hardware used by SRBL. SRBL's system can be divided into three general categories: the outdoor hardware, the indoor hardware, and the software.

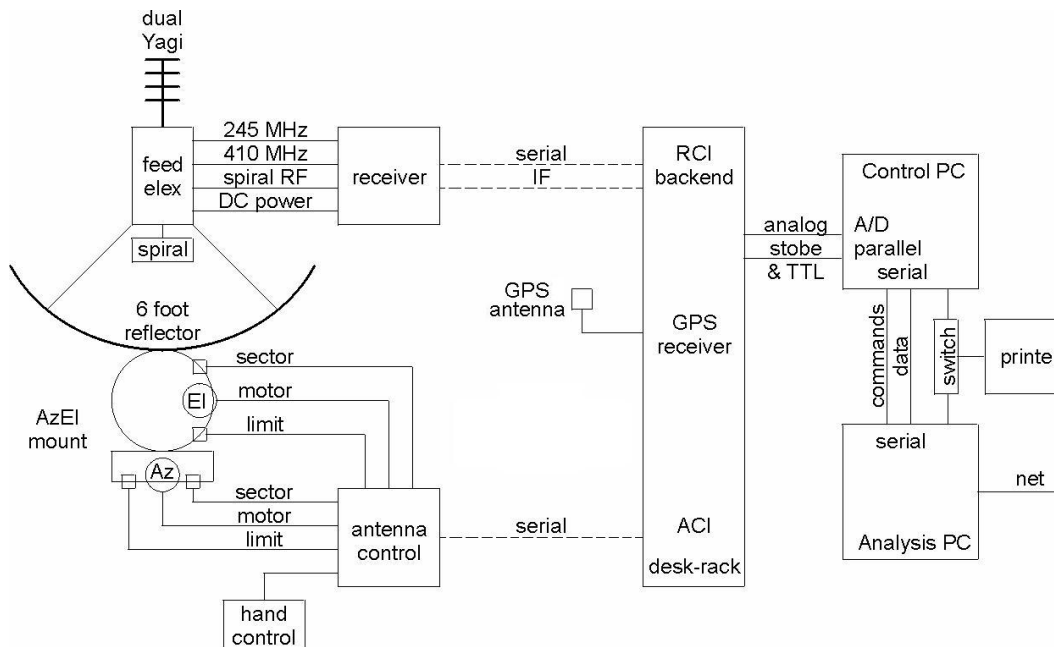


Figure 2-1 SRBL design schematics.  
 Courtesy United States Air Force.

### 2.3.1 Outdoor Hardware

SRBL uses a six-foot parabolic dish to reflect signals to the logarithmic spiral antenna that is mounted at the dish's focal point (see Figure 2-2). This antenna is designed to detect frequencies between 0.5 and 18 GHz. Additionally, a detachable dual Yagi antenna was added to be able to detect two sets of frequencies below this range. Those frequencies are 402-418 MHz and 240-250 MHz. The Yagi was added with the purpose of allowing SRBL to detect all of the frequencies covered by RSTN. Thus far, however, data from the Yagi has been unreliable, and because of this, operators of the Sunspot SRBL have often chosen to limit SRBL's observations to frequencies above 2 GHz.

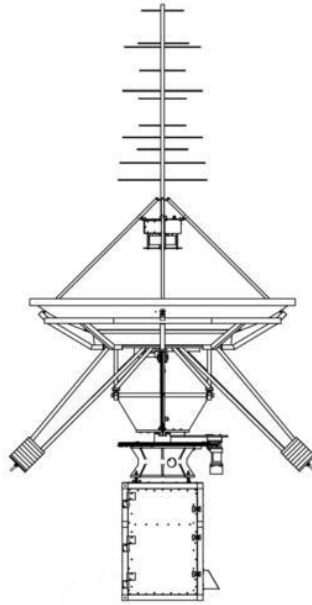


Figure 2-2 SRBL antennas.  
Courtesy United States Air Force.

SRBL's log-spiral feed is formed by two interlaced traces (see Figure 2-2). It is a quarter-wave, circularly polarized receiver that measures between 0.5 and 18 GHz [8]. However, it only attempts to find the burst locations for frequencies above 2 GHz and, by default, only those events that have an intensity above 500 solar flux units (sfu). However, this intensity threshold can be changed by the operator.

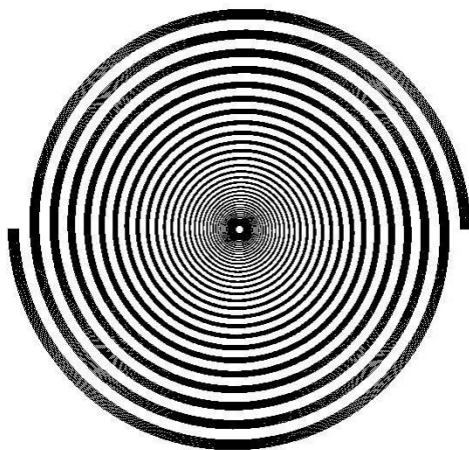


Figure 2-3 SRBL log-spiral antenna.  
Courtesy United States Air Force.

SRBL uses an azimuth-elevation mount, and its specific pointing is controlled by a 2-millidegree stepper motor and chain drive control [8]. The system is open-loop, and thus non-corrective during the course of a patrol. However, basic calibrations are automatically performed each morning before the beginning of the patrol, and more extensive calibrations can be run at the operators' discretion.

Timing information is obtained by means of an external global positioning system (GPS) unit [8]. The information obtained by this GPS is processed by SRBL's indoor hardware and software.

### 2.3.2 Indoor Hardware

All signals from the SRBL pedestal, the SRBL antennas, and the GPS unit are sent indoors where they are routed or processed by the electronics in the computer interface drawer. A bank of light emitting diodes (LEDs) and an audio speaker are

placed on the front of the drawer to provide basic diagnostic information for SRBL's operators (see Figure 2-4).

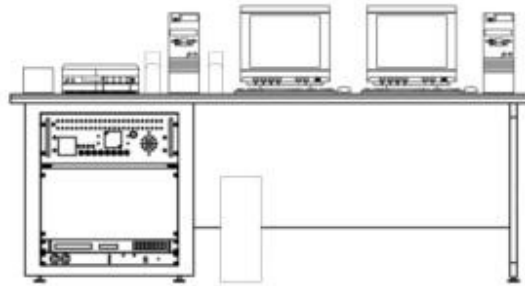


Figure 2-4 SRBL indoor hardware.  
Courtesy United States Air Force.

The rest of the indoor equipment consists of two computers with identical hardware. These computers are named Control PC and Analysis PC. Both of these systems have dual processors running at 733 MHz. Control PC is an MS-DOS® system that runs a Forth-based program to communicate with the SRBL pedestal. Analysis PC is a Microsoft® Windows NT™ system that provides a graphical user interface (GUI) to the Control PC. SRBL data is stored and viewable on Analysis PC.

### 2.3.3 Software

There are two primary built-in programs used to interact with SRBL and its data. LARC (Locating Antenna/Receiver Controller) is a low-level program that sends commands to and receives data from the SRBL antenna. LARC runs on the Control PC and is written in Forth and Intel® Assembly.

Although SRBL operators can directly enter Forth commands to interact with SRBL, a higher-level user interface is designed for this purpose and is executed on the Analysis PC. This GUI based program allows the user to send basic commands to the system and to view graphical representations of the data. Both real-time and historic data can be viewed. Patrols, calibration routines, and threshold modifications can be performed through the SRBL user interface.

## 2.4 Existing Functionality

This section presents an overview of SRBL's existing data collection, processing, and storage procedures. All SRBL data is collected using the processes described herein. It is important to have an understanding of these underlying processes before beginning to build a computational tool to analyze the data.

Each morning, before beginning its daily patrol, SRBL performs several pre-sunrise calibrations. During this time, SRBL pre-scans its path for any items that may be transmitting at frequencies that could cause interference. Examples of possible sources of interference include satellites and commercial broadcasts. After eliminating noisy frequencies, SRBL selects 120 frequencies between 500 MHz and 18 GHz to use throughout that day's scan. Users can also specify preferred and undesired frequencies. [8]

Once the Sun rises and a patrol begins, the 120 selected frequencies are cycled through twice every 9.6 seconds – once with a noise diode and once without. The noise diode helps with ongoing calibrations throughout the day. As data is collected, it is sent

first from the antenna to the Control PC, and then forwarded to the Analysis PC for storage and analysis.

When a new patrol begins, SRBL's built-in software generates an ASCII file for storing that patrol's data. The first several lines of the file provide basic information about the patrol. This includes such information as the year, the day of year, the location code, how information should be displayed, and the frequencies chosen for that run. Files are always 10,365 KB in size. The file size is forced at the time of file creation by adding extra lines with the phrase "-- FILL --" at the end of the file. As data is collected, it overwrites some of the "-- FILL --" lines.

Every 9.6 seconds, SRBL cycles through all of its frequencies twice - once with the noise diode, and once without. This block of information is stored in the data file for that patrol. In the block, the first piece of information recorded is the timestamp of the observation. Time is given in seconds since midnight UTC (Coordinated Universal Time). This is followed by the intensity readings for each frequency, followed by the intensity readings for each frequency with the noise-diode turned on. Since this file is meant to be human readable, each timestamp recording is displayed as a paragraph (not as a single line). The file is not committed to permanent storage until the patrol ends.

SRBL provides several methods for displaying collected data. Views are available for analyzing daily patrols, location attempts, and calibrations. The default display for viewing daily patrols uses a graph that provides information in three dimensions. The x-axis provides timestamp information, the y-axis lists frequencies, and the third dimension--signal intensity--is given by color. Several variants of this view



are available. Operators can choose to toggle scales between linear and logarithmic modes, switch to a three-dimensional view of the data, and show only a portion of a patrol.

The SRBL software also provides a method to chart individual frequencies. In this mode, only two dimensions of data are viewable -- time and intensity. These charts are available for every frequency chosen for a particular patrol.

When burst intensities are high enough, SRBL attempts to locate the source of the burst on the solar disk. This information is available to the operator in the form of a rough map of the Sun. The burst location is shown as a ring superimposed upon the map. The greater the uncertainty of the burst location, the larger the diameter of the ring. Only the last reading with a large enough intensity magnitude is shown in the image.

Some calibrations also provide graphical representations of the data they collect. These are generally shown in a form similar to patrol data: time along the x-axis, frequencies scan along the y-axis, and intensity given by color variation.

## 2.5 Goals for SRBL

There are numerous goals that have been described for SRBL since the time of its initial design. SRBL has been in operation for several years, and during that time some goals have been met, while others have been added, discarded, or altered.

Several of these goals are listed below. A brief description of the status of each goal follows.

Some of the primary goals for the SRBL project are to:

- Detect radio activity on the Sun
  - Detect microwave bursts that may cause communication interference
  - Determine locations of large bursts on the Sun
  - Provide continual monitoring of the Sun in the microwave spectra
  - Correlate activity with measurements from other instruments
  - Create a tool to search for user-specified bursts
  - Automate and simplify correlation process
  - Generate accurate nowcasts
  - Create forecasts of solar events
  - Use data to form predictions of solar radio events
- 
- Detect radio activity on the Sun

This task has been successful. Two SRBL units, one at Sunspot, New Mexico and the other at the Owens Valley Radio Observatory in California, have been collecting solar data for several years. Although SRBL has had various hardware and software problems that have interfered with its operation, it has been able to collect metrics for numerous frequencies, and both SRBL units have been able to detect and identify powerful radio bursts.

- Detect microwave bursts that may cause communication interference

SRBL has been successful in this area. When properly setup and calibrated, SRBL has been able to identify microwave bursts as they occur. There have been some instances of both false positives as well as false negatives. The false negatives

are generally due to the instrument having some type of hardware or software problem that prevents most spectra from being detected. Operators are usually aware of these problems at the time. The false positives have generally been caused by interference or by a sudden shift in baseline readings. This type of incorrect data is usually not predicted. However, by studying the characteristics of real bursts, better identification methods can be built into SRBL. This would allow SRBL to be able to provide more intelligent alerts when high intensity readings are measured.

- Determine locations of large bursts on the Sun

SRBL has the built in capability to locate the approximate source of solar microwave bursts. This capability is unusual for telescopes operating at radio and microwave frequencies. Typically, for instruments using these bands, locations are pinpointed by means of either mechanically moving the instrument back and forth while pointing near the source, or by means of interferometry. SRBL instead uses frequency responses across the log-spiral antenna to provide data for calculating locations. The higher the intensity readings, the more accurate SRBL tends to be in its location attempts.

- Provide continual monitoring of the Sun in the microwave spectra

SRBL was intended to be a network of units operating throughout the world so as to provide continual observations of the Sun. However, this goal was never attained due to the program being canceled before the production of all units was completed.

- Correlate activity with measurements from other instruments

On several occasions, the SRBL unit at the Owens Valley Radio Observatory (OVRO) has had studies performed on its data comparing its results with the results of

other instruments. In 2000, an evaluation was conducted comparing the data of the OVRO SRBL prototype, RSTN, and SOON [7]. As discussed previously, SRBL and RSTN are both radio telescopes operating in some of the same bands. When comparing the OVRO SRBL to RSTN, data correlation was high. "As a rule, all bursts recorded by SRBL were also seen by RSTN, and vice versa within live-time limits." [7] Later, in 2005, a similar study was performed that looked at both correlation of SRBL and RSTN data as well as the accuracy of SRBL location attempts. Correlation was again found to be high ( $r=0.9$ ), and location error for single source events was estimated to be about 4.7 arcmin [13]. No in depth study or analysis has yet been performed with the Sunspot SRBL.

- Create a tool to search for user-specified bursts

SRBL's software has the built in capability of viewing graphical displays of events as they happen and storing this information for later perusal. However, it does not have a way of searching for events that meet specific criteria. To find these requires either knowledge of when the event occurred or by using trial and error. My programs attempt to solve this by making events searchable. Such a task includes data mining, data analysis, and creating a useful human-computer interface. A basic understanding of the physical events that SRBL is reporting is also necessary.

- Generate accurate nowcasts

SRBL's built-in alert system is designed to inform operators of events as they occur. However, more can be done in this area to provide a fuller understanding of how a solar event may affect a multitude of systems. SRBL's data may eventually be included in the Solar Radio Burst Effects (SoRBE) system. SoRBE, which currently

uses RSTN data, was developed to combine information from solar radio monitors and various communication systems. The result is a method of identifying systems that may be adversely affected by a particular event.

- Create forecasts of solar events

As understanding of event characteristics grows, the amount of forecasting is expected to also increase. Short term predictions may include the duration, timing, and frequency drifts of an ongoing event. Eventually, longer term predictions are desired, and research is underway in this area. "Spectral signatures seen in microwaves often mimic the signatures seen in hard X-rays that lead to predictions of proton events in space." [16] By expanding our knowledge of the full spectral characteristics of solar events, it may be possible to find patterns, precursors, and early signs of bursts before they occur.

## CHAPTER 3

### ANALYSIS METHODOLOGIES

#### 3.1 Purpose of Analysis

This chapter explains the data mining and analysis methodologies performed on Solar Radio Burst Locator (SRBL) data for this thesis. There are three primary reasons for performing SRBL data mining and analysis.

First, up until this study, no in-depth research has been performed on the data collected by the Sunspot, New Mexico SRBL. Several studies have been performed on the data collected by the Owens Valley Radio Observatory (OVRO) SRBL, but the two systems are slightly different in their hardware and software, they are in different locations, and they operate amongst a different set of localized interference. The Sunspot SRBL has collected several years of data that before this research had yet to be analyzed.

Second, analyzing SRBL data helps to gain feedback on how well the SRBL system operates. By comparing data collected by SRBL to data collected by other instruments, a great deal can be learned about the quality of SRBL's solar microwave activity records. Additionally, knowledge can also be gained regarding what portions of the hardware and software function properly and what portions need improvement. This information can be taken into consideration when building future systems that use some of the same mechanisms.

Third, analyzing SRBL data can help us learn more about microwave bursts and can help lead to better understanding and prediction of these events. Software-based warning systems such as SoRBE (Solar Radio Burst Effects) could make use of SRBL data to improve nowcasts and warnings issued about solar microwave interference.

### 3.2 Method of Collection and Format of Data

As discussed in Chapter 2, SRBL selects 120 frequencies between .5 and 18 GHz for each day's patrol. Every 9.6 seconds measurements are taken at each of these frequencies with and with-out a noise diode. The 240 readings taken during this interval make up a single data sample. Each sample is recorded to a flat file that is available for viewing in its raw format and for software interpretation.

The SRBL software provides a user interface with a graphical representation of the data collected during a patrol. Several data views are available, but the primary format uses a two-dimensional heat map to show time (x-axis), frequency (y-axis), and intensity (color). An operator viewing the data with the SRBL software can also mouse over the image and read actual intensity readings at each x-y coordinate.

### 3.3 Analysis Methodologies Overview

Three methods of analyzing SRBL data are presented. The methodologies vary in complexity and focus, and they are presented in the order of increasing automation. The first method uses primarily manual techniques and provides information about the quality of SRBL's event observations. The second method uses a hybrid of manual and

automated methods to determine the feasibility of identifying true bursts versus other detected events. The third method uses a mostly automated method to find and characterize events. Results for each method are presented in Chapter 4.

### 3.3.1 Manual Analysis

Initial analysis was performed manually using SRBL data as it is visually presented to operators. The purpose of this first analysis was to determine how well SRBL's visual representation of events correlated to event reports from other instruments currently being used to detect solar bursts. The National Oceanic & Atmospheric Administration (NOAA) maintains a list of solar bursts detected by many different instruments operating at many different frequency bands. Reporting observatories include: Culgoora, Australia; Holloman Air Force Base, New Mexico; Palahua, Hawaii; Sagamore Hill, Pennsylvania; Learmonth, Australia; Ramey Air Force Base, Puerto Rico; San Vito, Italy; and the Geostationary Operational Environmental Satellites (GOES) spacecraft. These instruments collect data in the optical, x-ray, and radio frequency bands. [11]

To reduce the quantity of SRBL data processed manually, four selection criteria were used:

- Only dates between July 15 and December 31, 2004 were considered.
- SRBL had to be on a regular patrol and operating properly.
- Only dates on which SRBL detected an event measuring more than 50 sfu were considered.



- Only dates on which NOAA had records of activity that occurred during SRBL's patrol time were used.

The selection process reduces data consideration to those dates on which both SRBL and NOAA have event records of a significant magnitude. Thus, the data sets being compared are reduced to only those days that are likely to show event correlation.

The 2-dimensional intensity heat maps of each selected patrol were examined for periods of broadband increases in solar flux intensity (brightenings). Discounting horizon measurements, any brightening that was found to have an overall intensity greater than 20 solar flux units (sfu) was recorded. To ensure completeness, numerous milder brightenings were also included. The start time, end time, approximate intensity, and a brief description of the event were recorded for each brightening.

The NOAA solar data archive was searched for all recorded events that temporally overlapped any of the brightenings. Each overlap, no matter the intensity or the duration was recorded and then compared to the information gathered by SRBL. Because weak brightenings detected by SRBL were included in the search, there are a number of SRBL recorded events that do not have corresponding NOAA data. Results of the comparison process are discussed in Chapter 4.

### 3.3.2 Hybrid Method - Programmatic and Manual Analysis

The second analysis goal was to determine the feasibility of recognizing real bursts in SRBL's data versus other types of brightenings. This was done using a combination of manual and programmatic techniques. Events were programmatically

searched for in the data between March 23, 2004 and August 9, 2005. Data before this range was not used because before that time, SRBL was physically located in a different environment with different operating conditions. An image of each event was created by the program and these images were then evaluated and categorized manually.

For this phase of analysis, SRBL's raw solar flux unit intensity data was used. Before any analysis could be done, the data first had to be reformatted and cleaned. Reformatting was a simple process of removing superfluous "--FILL--" lines and ensuring that all data from a single sample was on a single line. Cleaning involved dealing with unknown data values and removal of outliers. At a single timestamp, data intensity levels outside of two standard deviations from the average of that timestamp were considered to be outliers.

After being cleaned, the data was divided into 10 subgroups based upon frequency. The first two subgroups included a range of 1 GHz, and each subgroup thereafter had a range of 2 GHz. This decision was made so as to separate data collected with different hardware components. Subgroup 0 included anything below 1 GHz and used both the Yagi and the spiral antenna for detection. Subgroup 1 included the range between 1 and 2 GHz and used only the spiral antenna for detection. See Table 3.1 for more complete information.

Subgroup	Frequencies	Antenna	Local Oscillator
0	< 1 GHz	Yagi/Spiral	1
1	1 - 2 GHz	Spiral	1
2	2 - 4 GHz	Spiral	2
3	4 - 6 GHz	Spiral	2
4	6 - 8 GHz	Spiral	2
5	8 - 10 GHz	Spiral	3
6	10 - 12 GHz	Spiral	3
7	12 - 14 GHz	Spiral	3
8	14 - 16 GHz	Spiral	3
9	16 - 18 GHz	Spiral	3

Table 3.1 SRBL frequency ranges.

From each subgroup, the highest intensity reading was found and encoded based upon the intensity's value. Intensities were encoded based upon a logarithmic scale as shown in Table 3.2. Such feature-discretization reduced the data set being worked with at any time to a manageable amount.





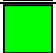
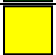




Code	Color	Value
0		No frequencies in range
1		Equal to 0 sfu
2		Less than 5 sfu
3		Less than 10 sfu
4		Less than 20 sfu
5		Less than 40 sfu
6		Less than 80 sfu
7		Less than 160 sfu
8		Less than 380 sfu
9		Equal or greater than 380 sfu

Table 3.2 Frequency subgroup color legend.

Using this reduced data set, active periods were searched for. If two consecutive timestamps were found to have at least two subgroups with a maximum intensity level greater than or equal to 40 sfu (codes 6 and above), then that point in time was marked as the beginning of an active period. As long as at least two subgroups were above 20 sfu (codes 4 and above), the event was considered to still be active. The event was considered to have ended when no activity rose above this level for at least four minutes.

A graphical image was created for each event using the coded values for each subgroup. Each value was assigned a color, and the start and end times were marked. (see Table 3.2 for color values) The event images included up to 15 minutes before and up to 4 minutes after each event.

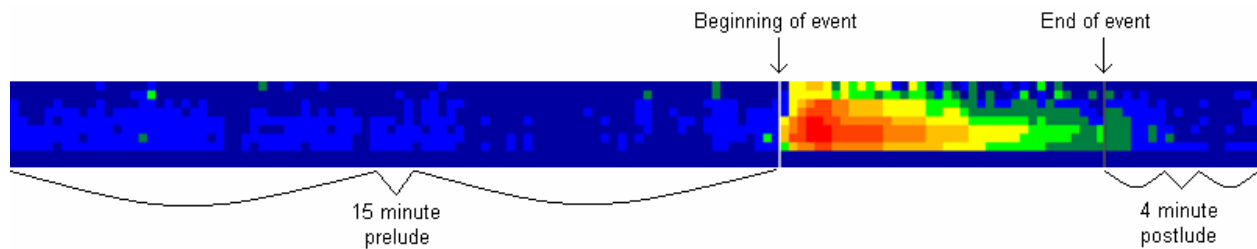


Figure 3-1 An event image.

Each image was then examined and categorized manually. Categories include *Blip, Early Morning, End of Day, Human Induced, Long, Probable Burst, Probable but Weak, Short, and Undetermined*. The classification methodology is based upon the subjective opinion of the human observer rather than strict objective rules. However, guidelines for categorization are as follows:

- *Blip* - Very sudden and brief increase in intensity, usually affecting a limited number of frequencies. Blips generally endured for no more than three samples.
- *Early Morning* - Broad spectrum brightening occurring during the beginning of a patrol. The duration of early morning brightenings varied, but they often lasted approximately one hour.
- *End of Day* - Broad spectrum brightening occurring during the final portion of a patrol. Duration of end of day brightenings varied, but they tended to last between 10 and 30 minutes.
- *Human Induced* - Brightening caused by some type of direct human interference. These tend to be of two types. The first is broad spectrum short bursts of interference with sudden starts and stops. The second is prolonged intense signals in a narrow frequency range. Most of the second type get classified in the *long* category.
- *Long* - Prolonged brightenings usually lasting several hours. These can be either narrow or broad band.
- *Probable Burst* - Brightenings that were likely to be genuine solar bursts. In most cases, these events had a period of growing intensity, a period of broad band high intensity (above 80 sfu), and a period of intensity falloff. The duration of the high intensity time varied greatly, but it tended to be for several minutes to close to an hour.
- *Probable but Weak* - Brightenings that showed all of the characteristics of a probable burst except that intensity levels were generally less than 80 sfu.

- *Short* - Brightenings that showed the characteristics of a probable burst except that their duration was very brief. These events usually lasted less than a minute.
- *Undetermined* - Brightenings that were not able to be easily classified by a quick visual inspection. Some of these were very noisy, some had many different events included, and some had errors in the data file. There were a myriad of reasons for an event to have an undetermined classification.

After an initial classification was assigned to each event, each was then checked against NOAA data to help determine whether or not it was an actual solar event.

Summarized findings for this process are given in Chapter 4.

### 3.3.3 Automated Method (Tool Development & Event Searchability)

The final method of analysis extended several features of the hybrid method described in subsection 3.3.2 and provided more in depth analysis of each event. Analysis included information regarding the duration of the event, the time of the maximum peak, the maximum peak intensity, and the frequency at which the maximum intensity occurred. Pictorial representations of each event were created just as in the hybrid method.

A summary analysis of all events meeting specified criteria was generated. This summary was used to provide general analysis of the variations in solar burst attributes.

To aid in this process, a software tool was created that allows users to specify specific attribute values rather than limiting the search to hard coded attributes. This tool is described in more detail in Section 3.4.

All events between March 25, 2004 and August 9, 2005 that met the following criteria listed in Table 3.3 were searched for. For each event found, the duration, the peak time, and an analysis for the peak time were found. The peak time analysis included average intensity, the highest intensity, and the highest frequency. The results of this analysis are given in Chapter 4.

<b>Parameter</b>	<b>Value</b>
Number of subgroups	10
Beginning - Intensity threshold	40 sfu
Beginning - Intense subgroups	2
Beginning - Consecutive intense timestamps	2
Ending - Intensity threshold	10 sfu
Ending - Intense subgroups	2
Ending - Consecutive intense timestamps	2
Ending - Maximum time below end threshold	4 minutes

Table 3.3 Event criteria.

### 3.4 Tool Development

The SRBL Online Data Analyzer was designed to simplify the process of finding solar microwave events that meet specific criteria. SRBL has built into it the ability to display graphical representations of events both in real-time and from the past.

However, a user wishing to find microwave bursts needs to either know when the bursts

occurred or must perform a manual search for them. There is not a simple method of quickly locating and viewing all recorded solar bursts.

One possible solution for this would be for SRBL to store a list of all bursts detected. Although this would aid in the problem mentioned above, it does not allow users to fine-tune the parameters to used. Only the events that SRBL has defined as bursts would be listed.

The tool described here is designed to be much more dynamic than this. Users can specify what intensity an event must reach to be listed. Users can also specify the frequency resolution of the image displayed, the amount of time before and after an event to show, the number of consecutive timestamps that must be above certain thresholds, and the dates to consider. All events meeting these criteria are then returned, and images and information about the event are then generated as needed by the user.

This tool was developed to be Web-based so as to be easily accessible to all those who have need for accessing SRBL data. SRBL is located in New Mexico, and most members of the Air Force Space Weather Center of Excellence are in Massachusetts. Further, team members may have need of sharing SRBL data with others located in various places around the globe.

### 3.4.1 Parameter Selection

Unlike SRBL's built-in user interface, the SRBL Online Data Analyzer has the ability to search for events above specified magnitudes. The searchability is controlled by parameters that describe characteristics of the event. These parameters include the



date range, the number of subgroups to divide frequencies amongst, intensities requirements, and the maximum amount of time between periods of activity.

The subgroups control the appearance of the event images generated. SRBL's total frequency range is divided by the number of subgroups and distributed evenly. If no frequencies in a particular subgroup were selected by SRBL during a patrol, that subgroup's row in the final image will be dark. Within each subgroup, the maximum intensity value (after the removal of outliers) is retained as the value of that subgroup.

This process has three implications. First, increasing the number of subgroups increases the frequency resolution of the final image. Second, reducing the number of subgroups reduces overall computation time. Third, changing the number of subgroups can affect the apparent start and end time of an event. This is because users can also select what percentage of subgroups must meet intensity requirements.

Intensity requirements are defined by the combination of several parameters. The minimum threshold is the solar flux intensity that must be crossed by a certain number of subgroups. Users are able to select both the threshold value as well as how many subgroups must be above this value. To further define the start and end points of selected events, users can select how many consecutive time samples must meet the other requirements. This option helps to reduce inclusion of noise spikes in the final results.

Solar events do not maintain a steady intensity levels over time. Thus, it is possible for an event to dip below defined thresholds for a period of time before again intensifying. For this reason, users can designate the maximum amount of time to allow for drops below thresholds.

### 3.4.2 Search Results

Results of the search are displayed in a hyper-linked list showing dates, start times, end times, and duration. Each event links to an individual page showing an intensity heat map and statistics regarding the event's peak frequencies, peak intensities, and duration. The event report is depicted in Figure 3-2.

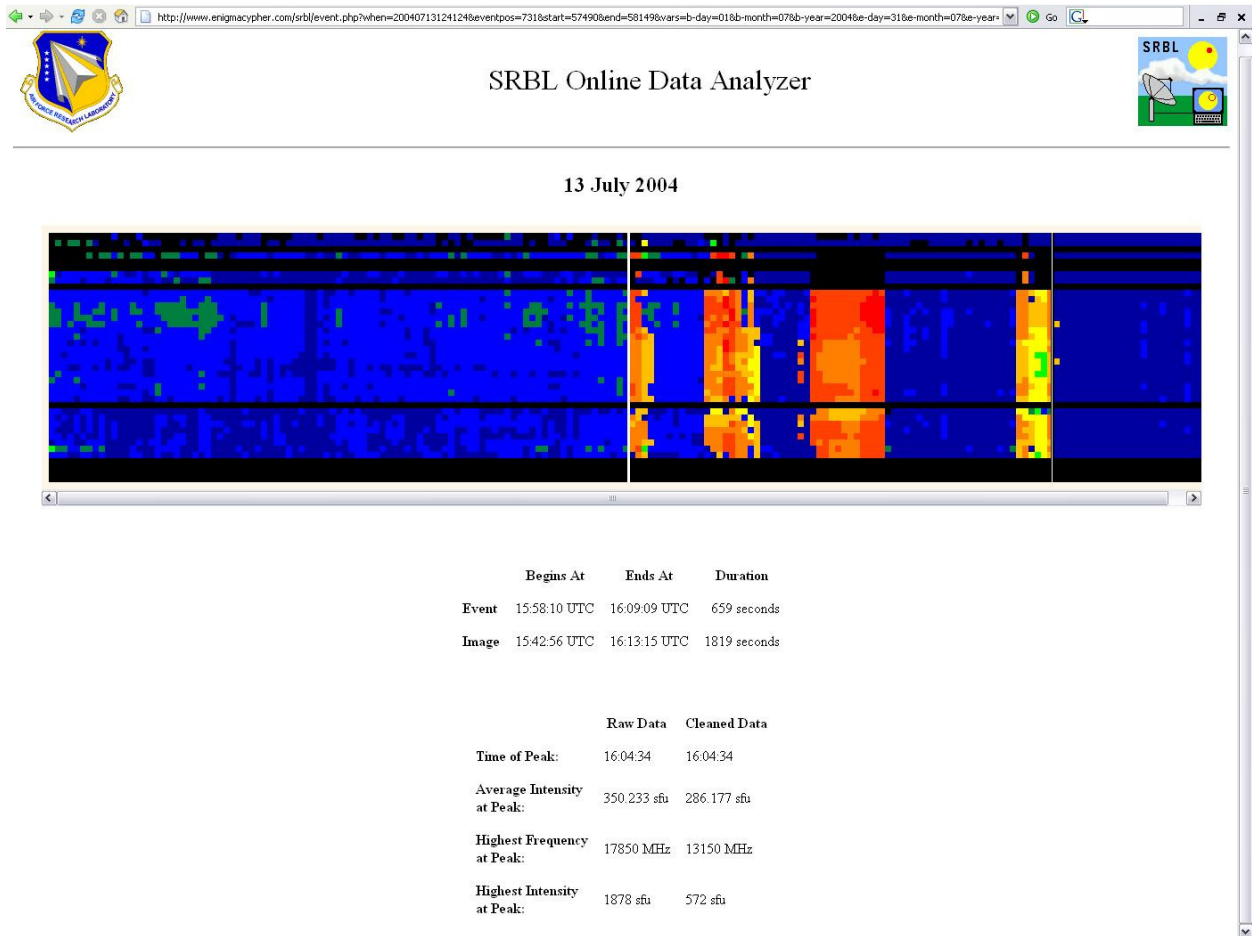


Figure 3-2 SRBL online data analyzer.

### 3.4.3 Summary Data

In addition to the individual event reports, three summary reports are created for download. Each of these reports presents data in as on all events returned by the search process. The 'summary of statistics' provides timing, duration, and peak intensity information. The 'summary of average intensities over time' lists the mean intensity for each sample of each event. The 'summary of intensities over frequency' provides data on the intensity average of each frequency for each event.

## CHAPTER 4

### ANALYSIS RESULTS

#### 4.1 Comparative Analysis of Instrumentation

As discussed in Chapter 3, the purpose of the manual analysis is to determine whether event data collected by the Solar Radio Burst Locator (SRBL) corresponds with data collected by other solar weather instruments around the world and in space. This information is necessary to know before proceeding further with data analysis.

To determine this, comparisons are made of data collected by SRBL on specific dates with data collected by several instruments that the National Oceanic & Atmospheric Administration aggregates. Data comparisons are limited to dates between July and December 2004 on which both SRBL and other instruments recorded significantly powerful solar activity.

A review of the data finds that during the selected dates, SRBL detected more than fifteen events registering above 50 sfu that were also detected by other instruments. Over three times this number of weaker events were also detected by both SRBL and other instruments. These findings are summarized in Table 4.1. Additionally, SRBL detected many weak events that were not reported in the National Oceanic and Atmospheric Administration (NOAA) archive. Only one brightening above 50 sfu was reported by SRBL that was not corroborated by data in the NOAA archive.

However, this brightening occurred at a time when SRBL was experiencing hardware problems and does not show characteristics common to most solar activity.

<b>SRBL intensity</b>	<b>Radio Only</b>	<b>Optical Only</b>	<b>X-Ray Only</b>	<b>Radio &amp; Optical</b>	<b>Radio &amp; X-Ray</b>	<b>Optical &amp; X-Ray</b>	<b>Radio, Optical &amp; X-Ray</b>
<b>&gt; 50 sfu</b>	1	0	1	0	10	0	6
<b>&lt;= 50 sfu</b>	28	2	14	2	11	3	9

Table 4.1 Number of events that corresponded with SRBL readings in various wavebands.

As might be expected, SRBL had the best event correlation with other radio telescopes. The next best correlation was with the x-ray instruments. Powerful events tended to show up in both radio and x-ray bands, and the most powerful events were usually detected across the radio, x-ray, and optical bands.

These correlations and conclusions are rough. The information provided by NOAA only tells of events that were reported. It does not provide information as to when each instrument is operational or what the lower threshold values are for reporting events. Therefore the results presented above should not be considered conclusive in comparing the ability of SRBL to detect events compared with other instruments. However, the results do show that the events that SRBL detects are corroborated by other instruments.

#### 4.1.1 Timings

A review was also made which compared the above events in their start times, end times, and overall duration. In general, the events seem to correlate in these parameters. Some differences were seen in the beginning and end times for the same events in various frequency bands. However, with-out knowing a) threshold limits defining the beginning and end of events for each instrument, and b) whether these instruments are fully synchronized, it is not possible to draw conclusive results regarding event timings. Even so, most events, were similar in the timing amongst the measurements.

#### 4.1.2 Intensity Comparisons

Figure 4-1 shows graphical comparisons between SRBL's intensity readings and the readings of the GOES-12 X-ray satellite. The data shown in this figure was collected on July 23, 2006 between 17:00 and 22:00 UTC. Times are vertically aligned to show temporal comparisons. As can be noted in the image, SRBL and GOES-12 recorded similar increases in solar activity at approximately the same times. Broad spectrum events are likely to show this type of correlation across the frequency spectrum. However, solar activity does not always show this type of broad spectrum uniformity.

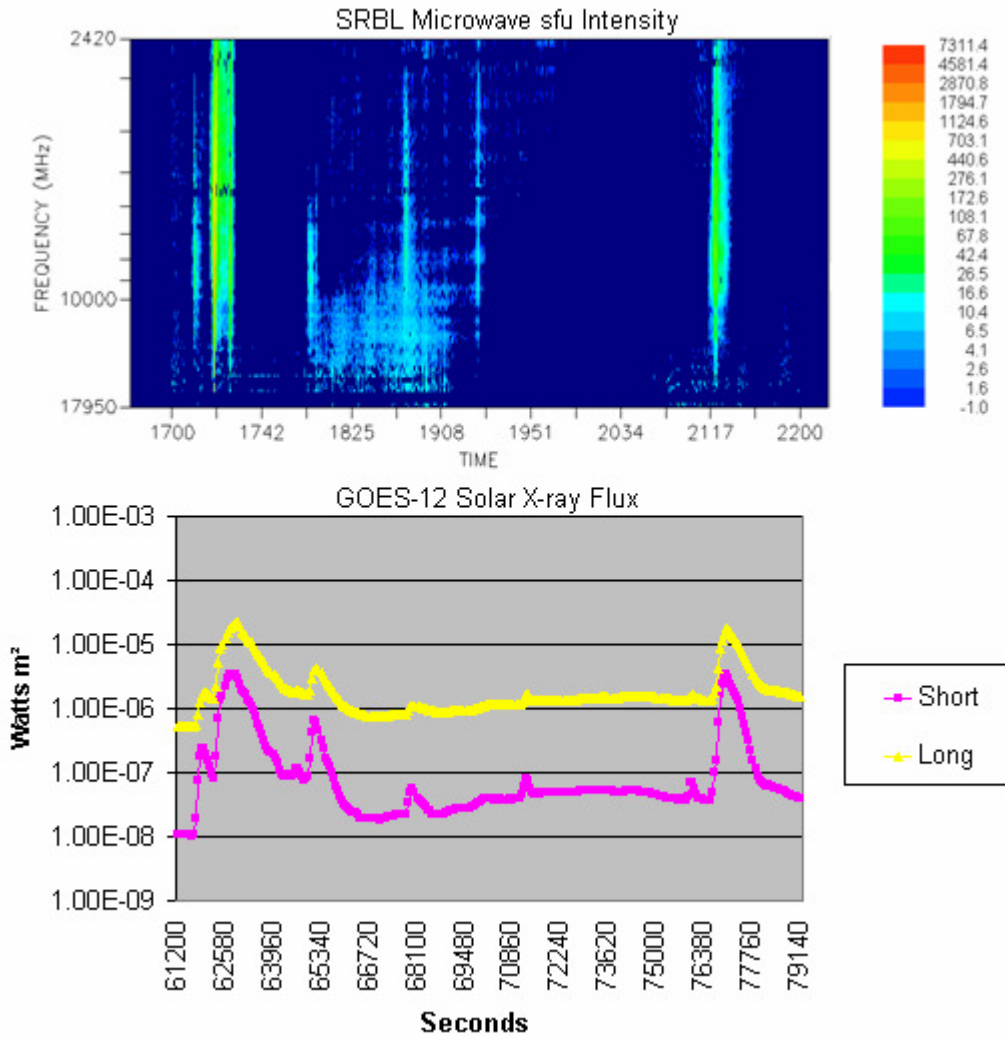


Figure 4-1 Graphical comparison of SRBL vs GEOS-12 readings.

Cursory comparisons were also made comparing SRBL intensities with measurements gathered by the Radio Solar Telescope Network (RSTN). However, the NOAA data archive only shows peak event values for RSTN. These values showed some correlation to SRBL data, but a more thorough analysis using the complete event data from both SRBL and RSTN would need to be performed to make any conclusive judgments on intensity comparisons.

In summary, this section has presented the results of the qualitative analysis performed to determine whether SRBL's detection of solar activity is in line with the measurements taken by other instruments. The analysis has shown that the events SRBL detects are both real and have similar characteristics to the measurements taken by other instruments. With this information, it is possible to move forward with more extensive event analysis.

## 4.2 Brightening Classification Analysis

This section presents the results of a comparison amongst many different types of brightenings detected by SRBL and seeks to determine the feasibility of separating real events from brightenings caused by various environmental factors.

Events were identified and images were generated following the data mining process described in 3.3.2. Events ( $N = 457$ ) meeting the selection criteria were analyzed, and each of these was individually reviewed to determine its categorization. Events were classified as *Blip*, *Early Morning*, *End of Day*, *Human Induced*, *Long*, *Probable Burst*, *Probable but Weak*, *Short*, and *Undetermined*.

### 4.2.1 Blips

Blips are very short brightenings with little to no intensity build up beforehand, and little to no intensity fading afterwards. Instead, there is usually a sudden increase above background level activity to activity registering high sfu values. The source of blips can vary. Sometimes they are caused by an electromagnetically noisy



environment, sometimes they are caused by hardware or software errors, and once in awhile they are indicative of an actual burst. Figure 4-2 depicts a typical data image of a blip.



Figure 4-2 Blip - June 24, 2004 - Duration: 0 hr, 0 minutes, 30 seconds.

Out of 457 events, nine events were classified as "blips". None of these were confirmed to be actual solar events, and seven were found to not overlap any events in the NOAA solar data archive for that time period. The two overlaps that did occur do not show good temporal correspondence with the NOAA records. In both cases the NOAA record begins well before the blip and ends well afterwards. Furthermore, both of these blips appear to be part of a noisy sequence of SRBL data.

Some solar microwave bursts are less than thirty seconds. However, solar bursts typically have periods of intensity growth and falloff and do not suddenly begin and end very high solar flux readings. This type of pattern is not shown amongst the blips recorded by SRBL. To be able to distinguish between noise and short duration events, an instrument with higher temporal resolution than SRBL would be necessary.

#### 4.2.2 Early Morning

The second event classification type is the early morning brightening. This is one of two types of horizon brightenings discussed previously. Typical early morning brightenings begin shortly after the beginning of a patrol, show a quick increase to

medium to high intensity readings, maintain this level of intensity across most frequencies, and then slowly begin to taper. A fairly typical early morning brightening is depicted in Figure 4-3.



Figure 4-3 Early Morning - July 23, 2004 - Duration: 1 hr, 19 minutes, 18 seconds.

Out of 457 events, 100 were classified as early morning brightenings. The duration of early morning brightenings varied between 9 minutes, 40 seconds to 3 hours, 2 minutes, 1 second.

During these brightenings, it is difficult to detect actual solar flux activity. Due to their long endurance many of these brightenings overlapped solar activity data archived by NOAA. However, none were found that corresponded well with the NOAA records.

#### 4.2.3 End of Day

End of day brightenings are the second type of horizon brightenings found in SRBL data. Upon examination, end of day brightenings have a similar, but reversed appearance to early morning brightenings. They tend to show a gradual build up to high, broad spectrum intensities, remain at this level for a while, and then quickly drop. Figure 4-4 shows a rather typical end of day brightening.



Figure 4-4 End of Day - July 11, 2004 - Duration: 0 hr, 8 minutes, 2 seconds.

A notable difference between early morning and end of day brightenings is the duration. For the most part, end of day brightenings are much shorter than early morning brightenings. The duration range was from 1 minute, 58 seconds to 38 minutes, 30 seconds. However, the shortest brightenings were ended not by reductions in intensity readings, but by SRBL's patrol completing. The shortest end of day brightening that was not prematurely cut off went for 2 minutes, 47 seconds.

Out of 457 events, 47 were classified as end of day brightenings. None of these events were confirmed to have been solar brightenings, but about 30% overlapped activity recorded in the NOAA archive. However, none of these were found to correspond well with the NOAA records, nor were there other indicators pointing to any of these brightenings being records of actual solar activity.

#### 4.2.4 Human Induced

The events classified as human induced were known to be caused by direct human interference. All three events occurred on July 13, 2004 during the testing of an RF shield designed to block interference from certain directions. A small hand-held radio was pointed directly at SRBL both from behind the shield and around it while SRBL was taking patrol measurements. The resulting readings showed very high intensity measurements that began and ended suddenly. An example of one of the test readings is shown in Figure 4-5.



Figure 4-5 Human Induced - July 13, 2004 - Duration: 0 hr, 6 minutes, 33 seconds.

#### 4.2.5 Long

The long category includes brightenings that last for more than fifty minutes that are not easily classified into another category. With-in this category, there are several distinct variants. Some, like the event depicted in Figure 4-6, have a very sudden beginning or ending and are likely the result of an instrumentation error.



Figure 4-6 Long - July 30, 2004 - Duration: 2 hr, 1 minute, 44 seconds.

Others, like the event depicted in Figure 4-7, show many characteristics of early morning brightenings. However, these events occur later in the day than those classified as early morning brightenings. Even so, it is possible that some of these are caused by the same source. More research is needed to determine the underlying cause of horizon brightenings. Once this is done, it may be possible to determine if some of the events categorized as long could be more specifically listed as early morning brightenings.

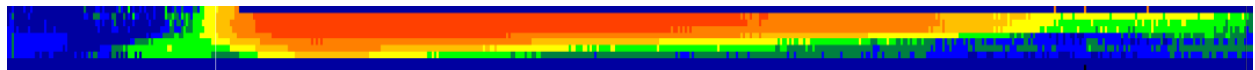


Figure 4-7 Long - February 1, 2005 - Duration: 1 hr, 12 minutes, 35 seconds.

A third type of event categorized as *long* were events that are noisy along a narrow band of frequencies. These events do not show any characteristics typical for solar microwave activity, but they produce enough intensity in enough frequencies to be selected for study. An example of this type of finding is shown in Figure 4-8.

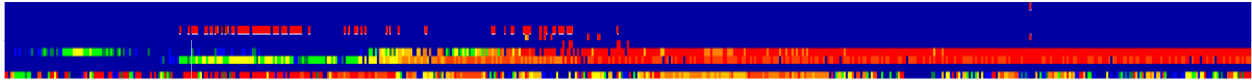


Figure 4-8 Long - March 7, 2005 - Duration: 1 hr, 23 minutes, 4 seconds.

Other events classified as longs included long durations of wide spectrum noise, periods of frequent but weak brightenings, and in a few cases brief activity embedded amongst long periods of weak brightening. A total of 52 events were classified as *long*. Due to their long duration, only 10 of these did not overlap any solar activity data in the NOAA archive. 6 others were found to include microwave bursts in their readings. The others overlapped NOAA archive data, but correlation with actual solar activity was not able to be verified.

#### 4.2.6 Probable Burst

The probable burst category includes events that show characteristics indicative of being a solar-induced intense brightening. These are the events that the Air Force is most interested in identifying so as to provide better warning systems for those that may be adversely affected by solar electromagnetic interference. These events tend to have a period of intensity build up, a several minute period of intense activity in most frequencies, and then a period of fading back to the normal background intensities for that day. To be classified as probable bursts, events had to have a maximum intensity greater than 80 sfu. Many events had sfu values greater than 380. Figure 4-9 shows a fairly typical example of this type of event.

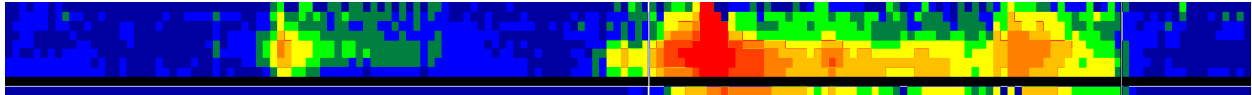


Figure 4-9 Probable Burst - July 23, 2004 - Duration: 0 hr, 10 minutes, 38 seconds.

Fifty events were classified as probable bursts. Of these, 24 were confirmed to be bursts, and 14 others showed some overlap with NOAA data records. The remaining 12 events were misclassified.

The misclassified events are the ones of greatest interest; for it is from these that the classifier definitions can be tweaked and honed. Of the 12 false positives, one appears to have been misclassified based upon the current ruleset. This particular event has a rather sudden beginning with the exception of a several frequencies that became intense well before the rest of the event. See Figure 4-10. If the start of the event had been considered the point where contiguous frequency subgroups crossed a threshold rather than any subgroups, then determining that the event did not meet the definition being used for probable bursts would have been clearer. The long duration of extremely high sfu values could also be used as a factor in reducing the identification of the event as a burst.

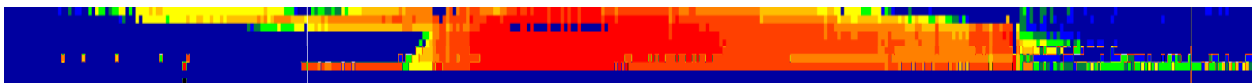


Figure 4-10 Misclassified as Probable Burst - August 8, 2004 - Duration: 42 minutes, 46 seconds.

Two other misclassified events had periods of quick broadband fluctuation in intensity readings. The root cause of these fluctuations is not known, but it likely caused by SRBL hardware malfunctions. During the time that these events were recorded, SRBL was experiencing problems that prevented it from passing its frequency

calibrations. Similarly, three other misclassified events appear to also be caused by SRBL malfunctions. The visual representation of these events appears to meet the criteria for being a burst. However, upon looking at the raw data, it is found that on the dates of these events, SRBL recorded negative flux values. These anomalous readings are indicative of hardware or software errors.

No clear reason has been found for the cause of the remaining false positives. These events meet the criteria for bursts, but other solar data archives do not show any events occurring during these times. Interestingly, half of the events in this group occurred on the same date, and the remaining events occurred with-in a week of that date.

#### 4.2.7 Probable but Weak

The probable but weak events show the same characteristics of probable bursts, with the exception that their maximum intensity is usually between 40 and 80 sfu. In the few cases in which sfu cross above 80 sfu, it only happens for a few seconds in a narrow frequency range. A typical example of a probable but weak event is shown in Figure 4-11.

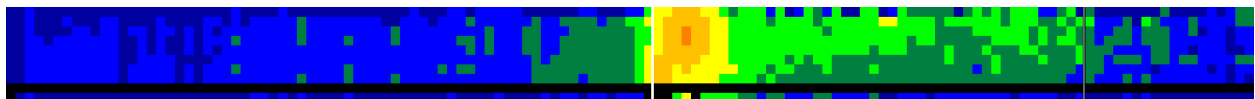


Figure 4-11 Probable but Weak - July 18, 2004 - Duration: 0 hr, 7 minutes, 22 seconds.

Forty-eight events have been classified as probable but weak. Most of these have a duration between 5 and 30 minutes. The shortest event in this class lasted for 1

minute, 58 seconds, and the longest lasting event in this class endured for 1 hour, 29 minutes, 47 seconds.

Of the 48 events, only 7 corroborated with records found in the NOAA archive. 21 were found to not be solar activity, and the rest overlapped some NOAA records but did not show strong correlation. The reasons for so few events being found to be of solar origin includes the reasons listed in Subsection 4.4.6 for probable bursts (noise, SRBL malfunction), and increase in mild readings being included in the data, and a reduction in the reporting for weaker events.

#### 4.2.8 Short

Events classified as being short showed all of the characteristics of bursts but on a rather rapid timescale. All of these events, save for one, lasted less than 3 minutes, 40 seconds. The one exception has a recorded duration of 12 minutes, 57 seconds, but almost all of this is in a prolonged taper at low intensities. The powerful portion of this event also only endured for around a minute. Figure 4-12 illustrates a fairly typical short event.

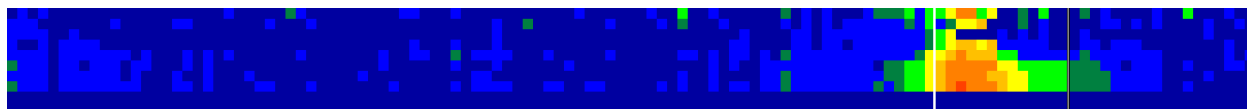


Figure 4-12 Short - July 14, 2005 - Duration: 0 hr, 1 minute, 58 seconds.

Only ten events were classified as being short events. All ten were confirmed as being caused by real solar activity.



#### 4.2.9 Undetermined

There are many different reasons for events to be listed in the undetermined category. Some events are excessively noisy. Some are somewhat long in total duration and include several different types of events with-in the whole. Some have data errors. Others may belong in one of the other categories, but a brief inspection did make this evident. In several instances new possible categories have been identified with-in the undetermined group. Adding these categories helps create stronger rulesets for identifying types of events. However, it should be noted that out of 138 events in the undetermined group, only 4 were found to be bursts, and 2 others showed strong indicators of including a burst with-in the dataset. 60 had no overlap with any NOAA solar records.

In Figure 4-13, an example of a noisy undetermined event that includes negative flux readings in the raw data is shown. Over a several month period, several of these events were recorded.

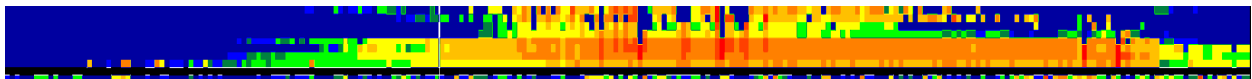


Figure 4-13 Undetermined - April 29, 2005 - Duration: 0 hr, 27 minutes, 12 seconds.

#### 4.2.10 Classification Summary

The classification system described above provides insight into various forms that SRBL event data typically can be grouped into. It shows that most real bursts can be identified. Currently, most of these are found in the categories of probable burst,

probable but weak, and short. By studying the characteristics of the true positives, the false positives, the true negatives, and the false negatives with-in each category, it is possible to refine the definitions of what true solar bursts look like to SRBL. In some cases, such as the horizon brightenings, it is important to discover the underlying cause for the brightening. This information can then be applied to other events thus strengthening the definitions. Over time, with more data samples, more conditions, and more environmental changes, it should be possible to identify real bursts with high reliability as they occur. The goal is to eventually be able to identify these events at their earliest stages to be able to provide reliable and timely warnings of solar microwave interference.

The research presented here has shown in a preliminary form that it is possible to identify most solar bursts by viewing only a reduced portion of SRBL's data set. The remaining analysis presented builds upon this information to provide a statistical view of solar microwave activity.

### 4.3 Analytical Metrics

This subsection discusses the results of several statistical methods of analyzing events detected by SRBL. Each of the events analyzed were identified by means of the Web-based software tool described at the beginning of this chapter. For Subsections 4.4.2 through 4.4.4, forty-three confirmed solar events were studied. Analysis of these events includes comparisons of event duration, temporal intensity mappings, and frequency vs. intensity analysis.

### 4.3.1 Duration Analysis

One characteristic of a solar event is how long it lasts. Although events are known to occur through-out a wide spectrum of time, it is interesting to determine whether the duration of microwave events detected by SRBL are equally distributed or whether certain durations are more common.

To determine this, forty-three confirmed solar events are studied. The duration of these events is shown in a histogram in Figure 4-14.

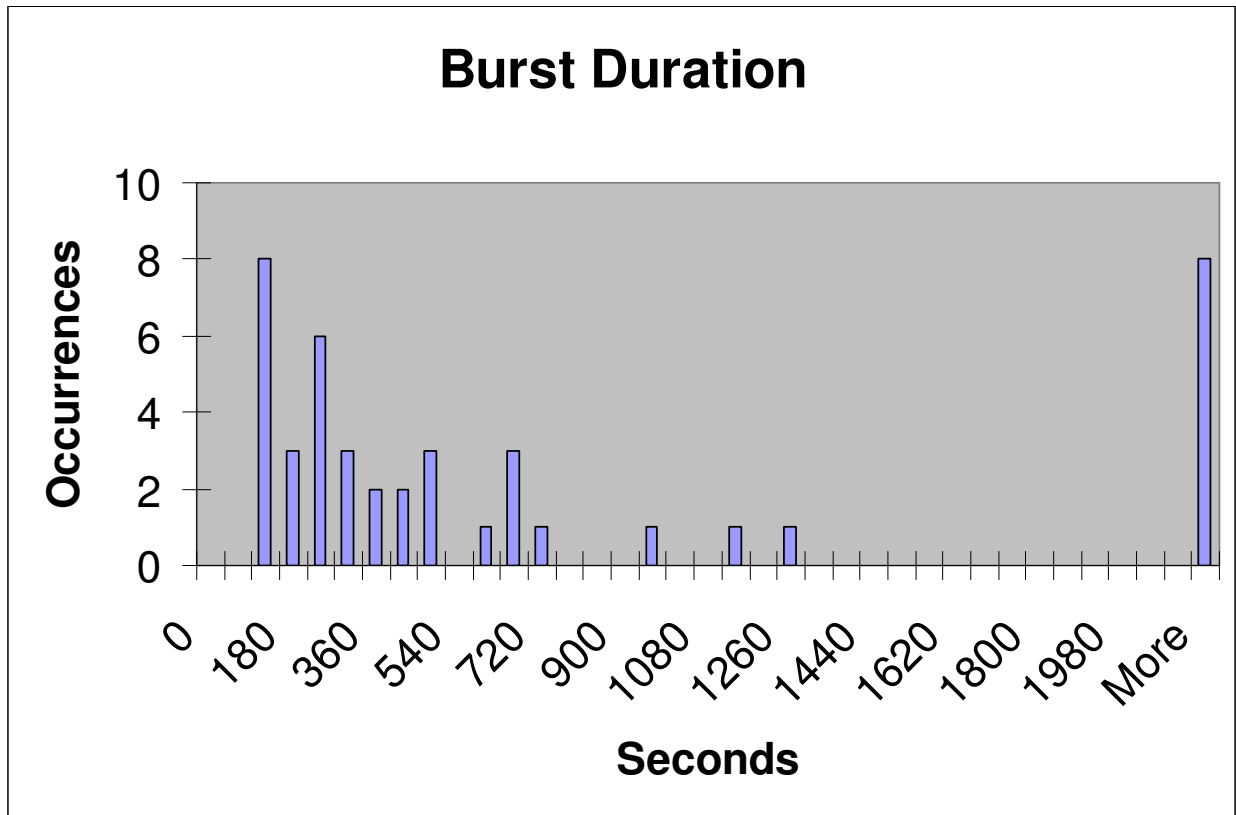


Figure 4-14 Solar event durations.

As can be seen, most events (63% in this case) last less than nine minutes. Event duration continues to drop off after this point with another 19% completing before the first half-hour is over. However, a significant number of bursts (19% in this case)

endure for more than this amount of time. Studying these longest events reveals some interesting information.

To determine the reason for a long event, it is important to review the raw, pictorial, and statistical data for each event. Doing this has revealed three distinct reasons for solar events to be recorded as lasting more than thirty minutes.

One of the events that is recorded as having a long duration is actually a rather short burst. However, it has a very long tail with intensity values measuring just above the ending threshold requirements. This event is shown in Figure 4-15.

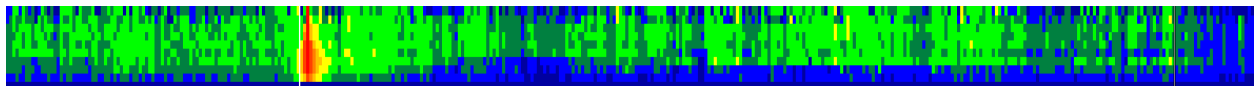


Figure 4-15 Short burst with long tail - November 8, 2004 - Total duration: 0 hours, 45 minutes, 13 seconds.

Five of the eight long lasting solar events are actually composed of multiple events that occurred very near to each other in time. Three of these consist of several bursts measuring more than 160 sfu at each of their peaks. The other two include multiple, weaker events.

The remaining two events are in fact verified bursts with uninterrupted high solar flux measurements that endured for a prolonged period of time. However, this is not to say that these events were the result of a single solar event. In fact, both these events show signs of including multiple bursts. The November 9, 2004 event is shown in Figure 4-16. Although the burst activity is uninterrupted, several intensity peaks occur during the event. Another interesting aspect of this event is the sudden end of intense activity. Further studies could be made on this event to determine whether the multiple

peaks are in fact multiple bursts and whether the event really did have such a sudden conclusion. The July 7, 2005 event will be discussed in more detail in Subsection 4.4.6.

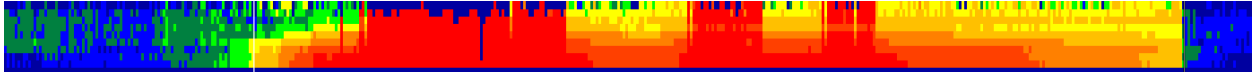


Figure 4-16 Long burst with multiple peaks - November 9, 2004 - Duration: 0 hours, 56 minutes, 31 seconds

#### 4.3.2 Burst Time vs. Intensity Analysis

In addition to looking at the total event duration, temporal analysis can be made on the intensity values through-out an event. For this, the average solar flux measurements at each timestamp were plotted, and the results showed the overall intensity shape of the burst. Figure 4-17 depicts the same event shown earlier in Figure 4-9 as an example of a probable burst.

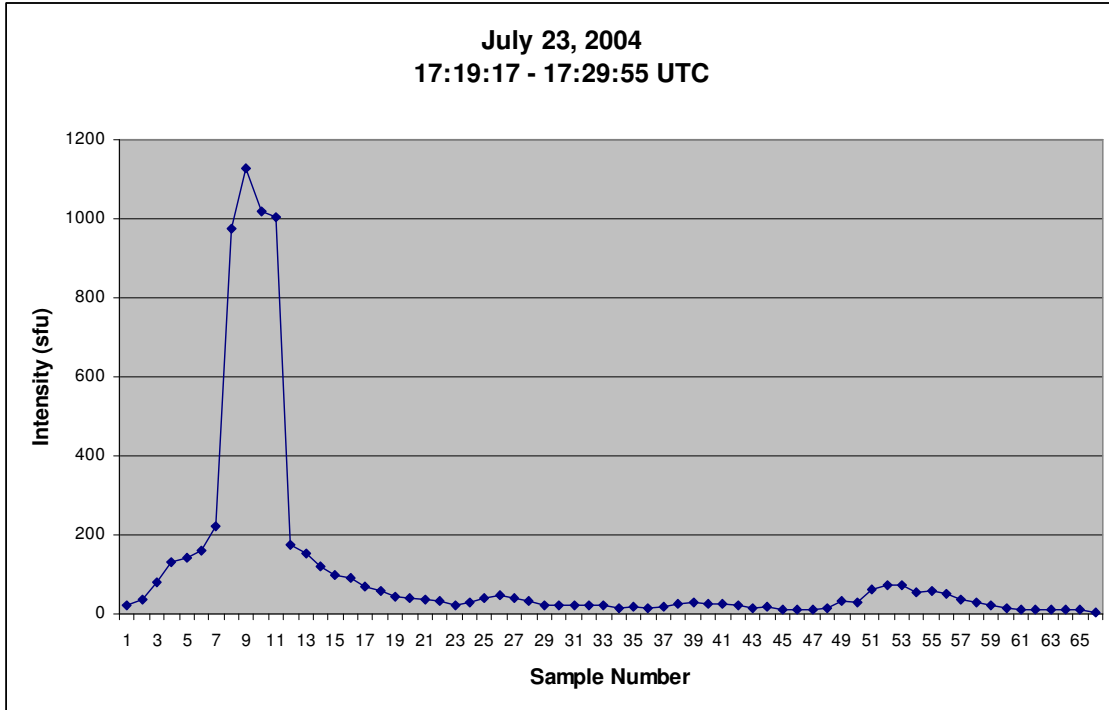


Figure 4-17 Intensity curve.

Viewed logarithmically in Figure 4-18, the similarity to the heat map representation becomes more evident.

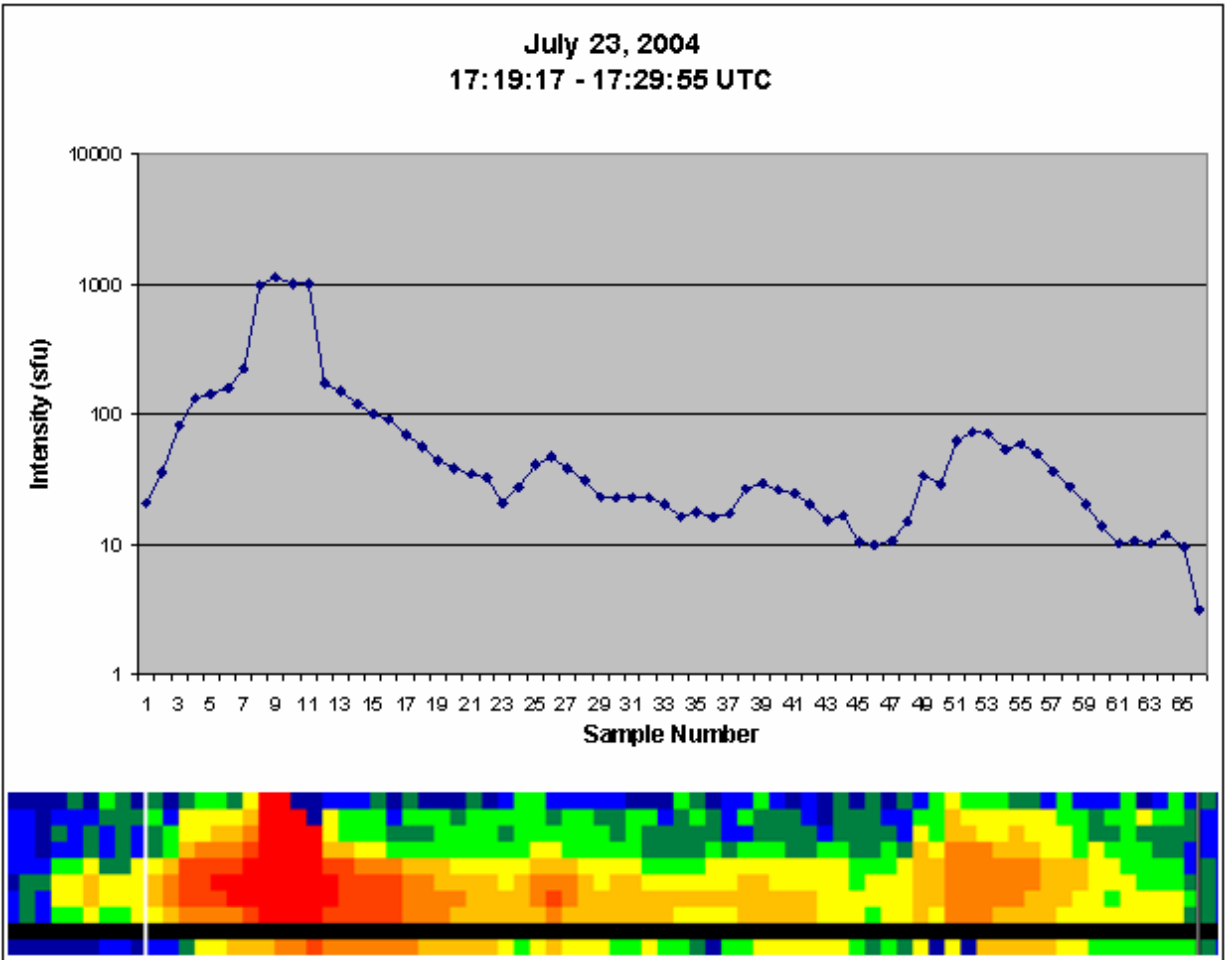


Figure 4-18 July 23, 2004 - Intensity comparison.

Studying an event's average intensity over time provides us the basic shape of the intensity curve. This presents the question of whether most solar microwave bursts have the same intensity curve characteristics. By comparing intensity curves of many events, this question can be addressed. Figure 4-19 shows layered plots of several solar microwave events. The start point of all events begins at sample one, and most of the events end well before sample fifty (or approximately 8 minutes).

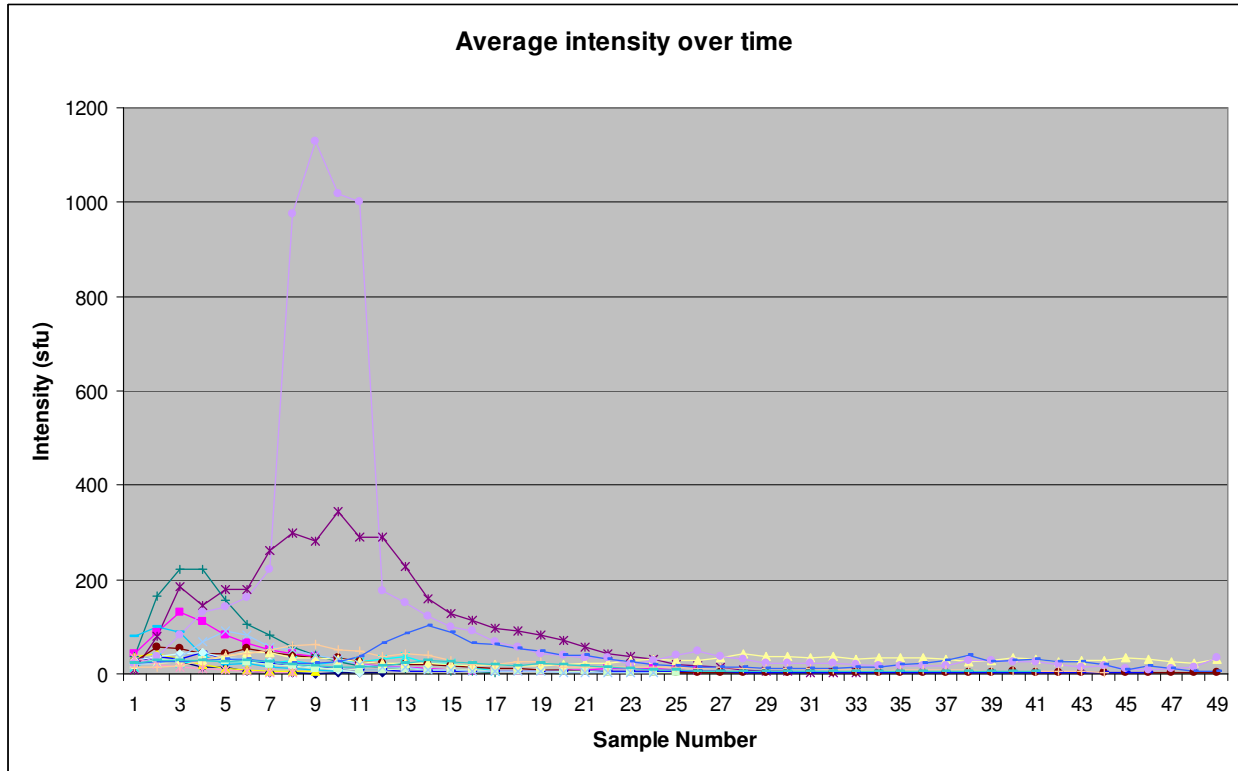


Figure 4-19 Average intensity over time.

Figure 4-19 gives the appearance that bursts reach their peak within the two minutes and then decline at a slower rate until finally tapering off. However, if all 43 confirmed solar events, including those with a long duration, are included in the plot, it quickly becomes evident that this initial assessment needs revising. As can be seen in Figure 4-20, many of the longer and more powerful events have a prolonged gradual growth period before beginning their major ascent. Most events have a fairly short time at their peak and then begin their decay period.



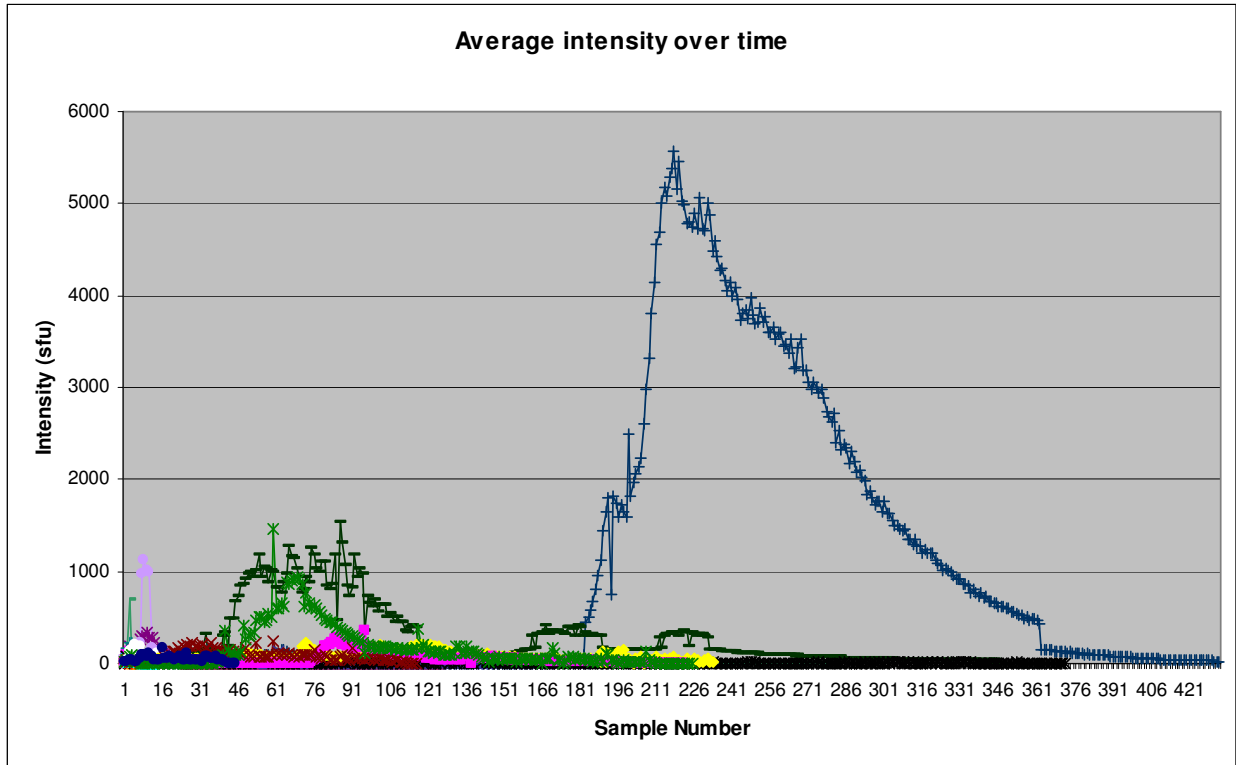


Figure 4-20 Average intensity over time.

#### 4.3.3 Burst Frequency vs. Intensity Analysis

Thus far events have been viewed primarily as functions of time and intensity. A third view is to look across the frequency domain. By taking the average of all values at the same frequencies throughout an event, it is possible to plot the peak frequencies a particular event. It is important to note that this information does not necessarily provide an accurate view of the frequency curve of the actual solar event. Rather, it depicts the frequency curve as detected by SRBL. Environmental factors, including interference, atmospheric distortion, and mechanical sensitivities may affect the shape of the overall curve.

One application of studying the frequency curves is to determine if there is a particular shape common amongst many microwave bursts. Shown in the figures below are two solar microwave events from 2004. As can be seen, these events have very different frequency curves. The first event is primarily concentrated in the mid-range frequencies, while the second event is centered on the lower frequencies. However, to make a true comparison, the actual frequencies used in each patrol would need to be compared.

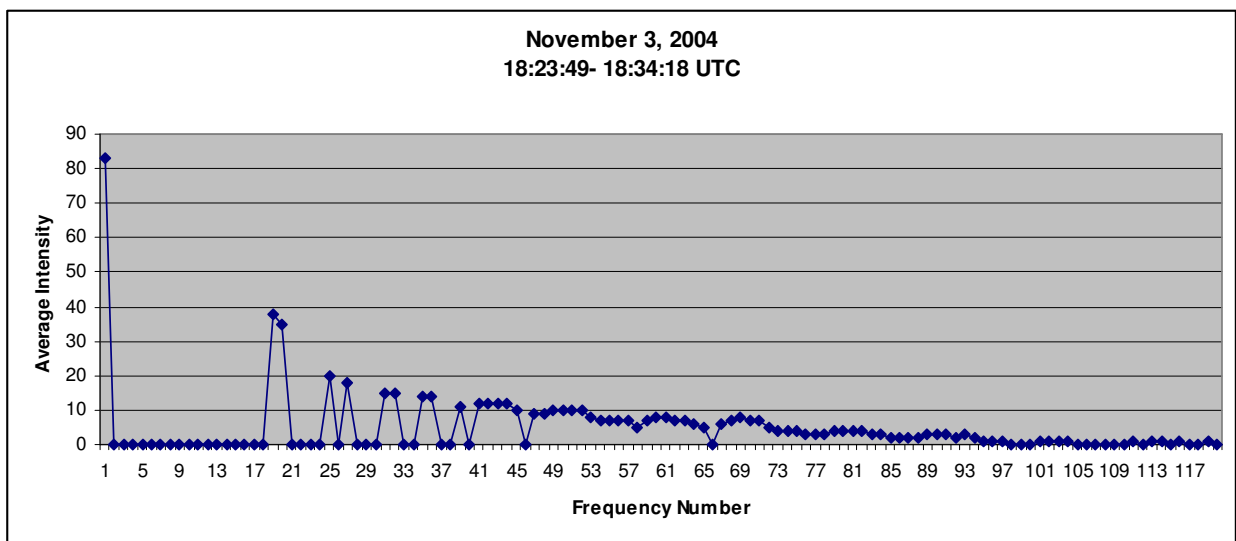
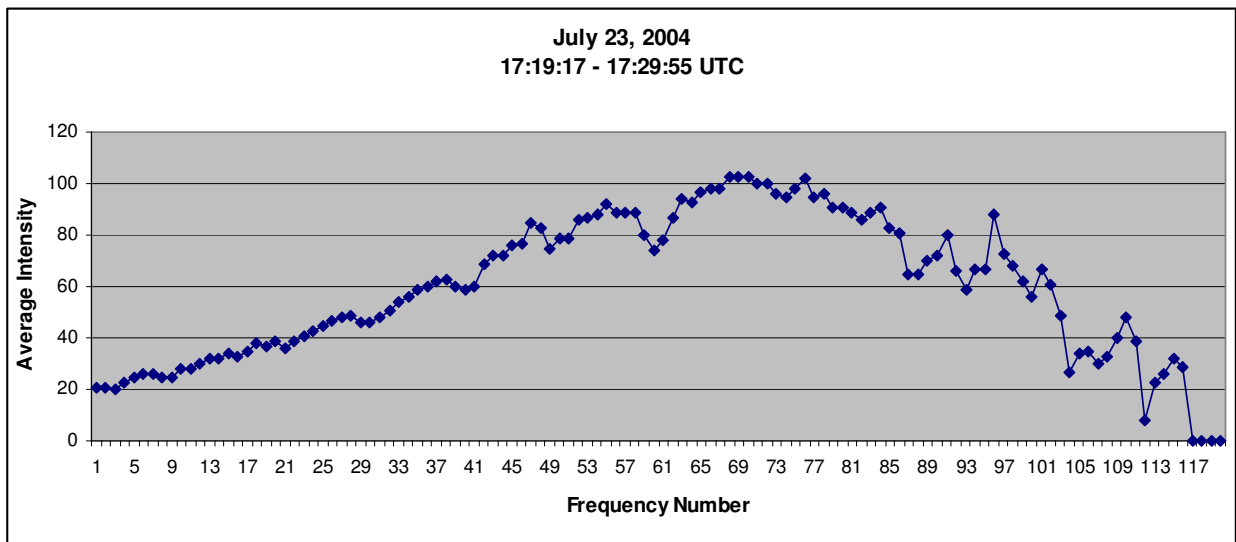


Figure 4-21 Frequency intensities.

### 4.3.4 Temporal Analysis of Horizon Events

On many days SRBL recorded brightenings at the beginning and end of its patrol. These horizon events have been determined to not be caused by increases in solar flux activity. Before a determination can be made as to the source of these brightenings, the events themselves must be studied.

A temporal comparison of the start and end times of each event has been made. In Figure 4-22 the recorded early morning brightenings from March 2004 to August 2005 are shown. The figure shows the start and end times for the events themselves as well as for the images as a whole. Since multiple years of data are included in the study, only the day of the year is considered in the time series.

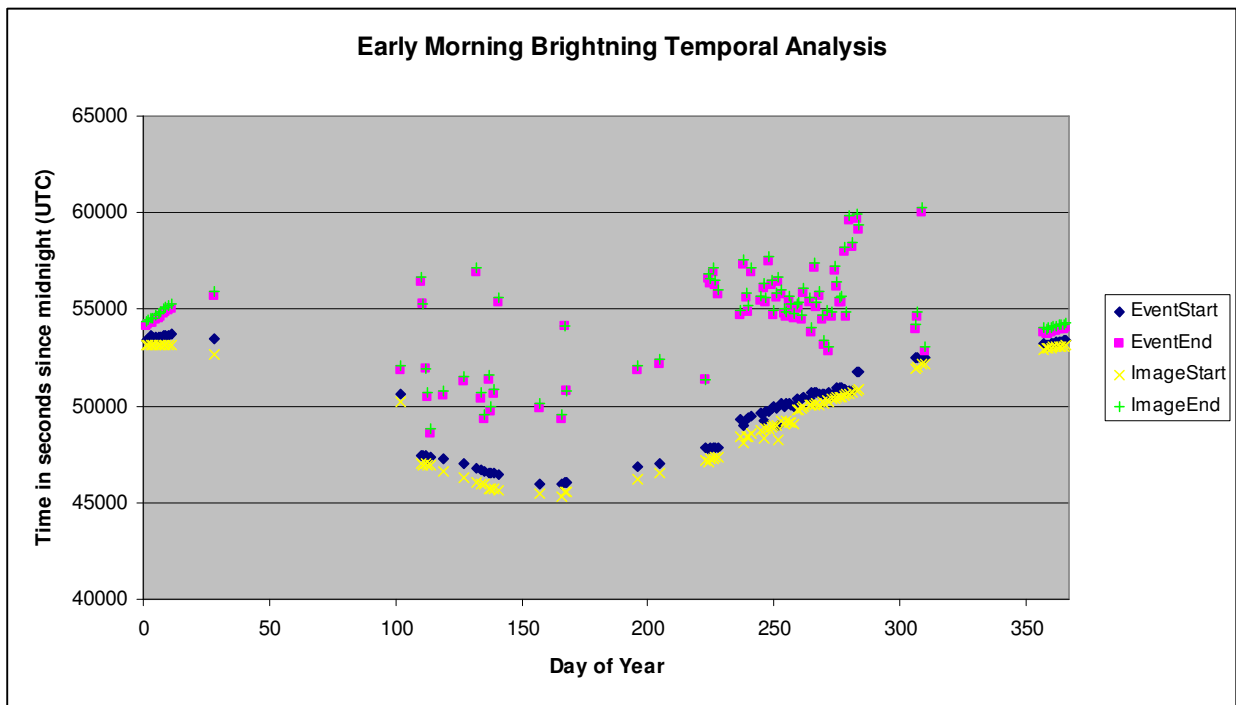


Figure 4-22 Early Morning brightening temporal analysis.

As can be seen, the start time of the events follows a sinusoidal pattern, beginning later in the winter months, and earlier in the summer. This is consistent with expectations as SRBL's patrol must also begin earlier during the summer and later in the winter due to the changes in sunrise times. However, if this were the only factor, one would assume that the latest start time would be at the Winter Solstice around December 21. However, the start time peaked at its latest on January 11, 2005. Further studies are necessary to determine the reason for this.

The end of day brightenings do not at first seem to follow the same type of distinct pattern. However, they do cluster during the summer, with the first appearing on May 20 and the last appearing on July 22. With these dates in mind, it is possible to note that events that end the latest occur in mid-summer, as would be expected. The sparsity of the data precludes absolute determination of the pattern. Whether the sparsity is due to coincidental effects or is in of itself a clue to the cause of the brightening requires additional investigation.

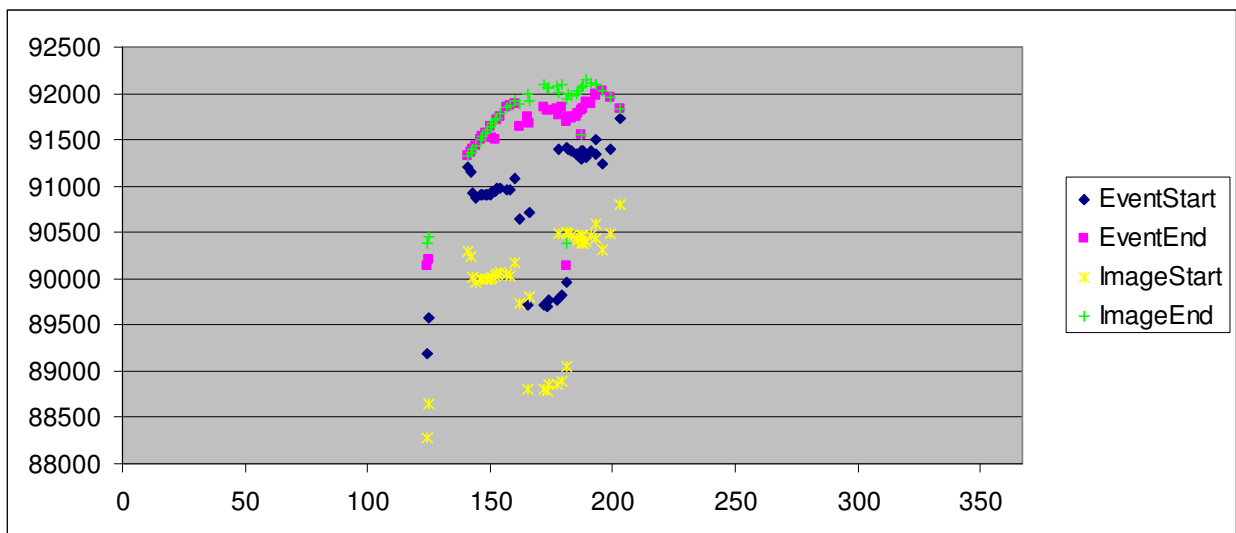


Figure 4-23 End of Day temporal analysis.

#### 4.3.5 Other Findings

During the process of sifting through and analyzing data, several unexpected discoveries were made. The discoveries themselves are beyond the intended scope of the research for this thesis, and therefore the information found has not yet been applied to the data set as a whole. However, it is hoped that these isolated findings can be used as building blocks for future research.

One of these discoveries was made because of the long lasting burst that occurred on July 7, 2005. This event, shown in Figure 4-24, does not show many of the characteristics common to most solar activity. The burst begins rather abruptly, maintains high sfu values at a very wide spectrum for a prolonged amount of time, and ends very suddenly. Such characteristics have been caused on occasion by a SRBL malfunction. Therefore, when this was first viewed, it was thought to be a recording error.

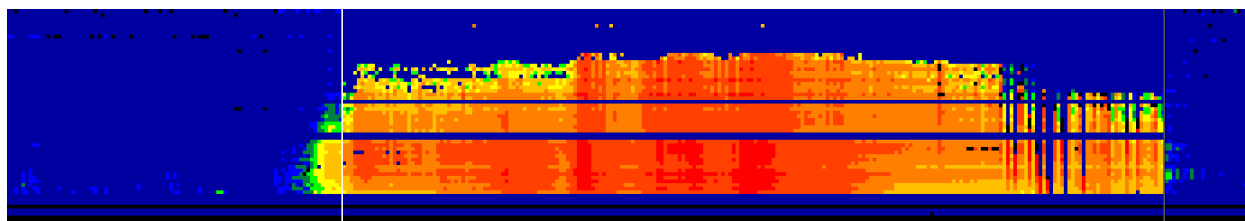


Figure 4-24 July 7, 2005 - Duration: 0 hours, 38 minutes, 1 second.

Note: To help provide feature detail, this event is shown with 60 subgroups rather than 10 as other events have been shown.

However, once this event was compared with GOES-12 x-ray data, it became very clear that this event was indeed the result of a solar burst. This event was also

powerful enough that SRBL attempted to locate where on the solar disk this event occurred. For this event only, a study was made of the location data that SRBL recorded.

Throughout most of the event, SRBL claimed that the burst was occurring at the Sun's north pole (see Figure 4-25A). This was known to be a fallacy since bursts generally occur at no more than  $\pm 45^\circ$ , and they are found much closer to the equator at the point of the solar cycle during which this event occurred. However, since this event was of such great magnitude, it was a simple matter to check with optical solar telescopes to verify that the eruption was coming from region 0786, near Sun center.

While perusing SRBL's location reports for this event, a few records were found that showed the burst being located along the Sun's north eastern limb (see Figure 4-25B). By applying a similar offset to this reading as was applied for the previous, it was found that the event appeared to be coming from region 0789. With the exact timestamp of this reading along with the location information, the ISOON optical telescope data was reviewed. ISOON revealed that during the time that the primary burst was erupting at region 0786, a secondary burst was also occurring at region 0789 at the point in time indicated by SRBL. This secondary event was not recorded in the NOAA archive.

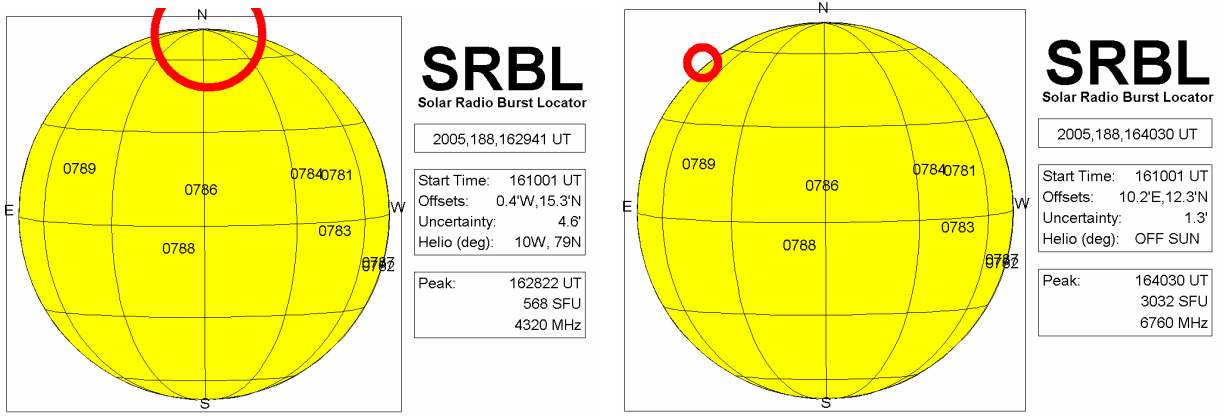


Figure 4-25 SRBL burst locations for simultaneous events.

Sympathetic bursts are not uncommon. The magnetic fields of sunspot regions are intertwined, and thus the changes at one location sometimes cause other effects across the solar disk. SRBL's ability to detect even a few of these sympathetic bursts is an improvement over what has traditionally been possible at microwave and radio wavelengths.

## CHAPTER 5

### SUMMARY AND CONCLUSION

#### 5.1 Summary

The Solar Radio Burst Locator (SRBL) provides a wealth of unmined data for solar spectra between .5 and 18 GHz. By applying data mining techniques, the information contained within this data can begin to be tapped. From this, determinations can be made about the functionality of the SRBL system and more can be learned about the characteristics of microwave bursts.

This thesis has viewed SRBL microwave data from several dimensional perspectives. An initial analysis was made comparing the timing of events recorded by SRBL to the events recorded by other instruments around the globe. This was followed by comparing these same events in the frequency domain to determine which spectra outside of the microwave bands that SRBL's data best correlates with. A look was then taken across intensity dimension to determine if SRBL's intensity readings were in line with the intensity values reported by other instruments.

Two dimensions, time and intensity, were used to provide a preliminary classification schema for events with consecutive samples measuring more than 40 sfu in at least two frequency subgroups. Nine event classes were created, and it was found that events matching the guidelines for the probable burst, probable but weak, or the short category were the most likely to be caused by solar activity.

The events that were confirmed to be caused by solar activity were further studied and compared with each other. Analysis was done on these events in the time



domain by comparing overall event duration, in the time and intensity domains by plotting the intensity curves, and in the frequency and intensity domains by plotting frequency curves.

## 5.2 Future Works

The analysis presented in this thesis lays the groundwork for additional studies to be performed upon the Solar Radio Burst Locator data. Several analysis techniques used in this work could be expanded. Combining various domains of analysis into the classification system would help provide better definitions of detected events.

### 5.2.1 Analysis Enhancements

Expanding upon the analysis techniques used thus far would produce additional information about the nature of solar events. For example, normalizing the intensity curves could show whether specific event types have recognizable signatures. Similarly, the work on the frequency domain could be expanded to include temporal comparisons to see if any microwave events have characteristic frequency drifts over time.

### 5.2.2 Classification Enhancements

The analysis performed thus far has looked at the three primary dimensions of the SRBL data and has shown that solar events tend to have many shared characteristics. This research can be built upon to further solidify classifications so that early identification of solar bursts can be made.

The classifications set forth in this work are based upon qualitative human judgment. Guidelines have been set forth, and based upon the results it should be possible to quantify the guidelines. Additionally, intensity and frequency curves could be made part of the classification schema.

### 5.2.3 Precursor Study

After the classification system is well established so that it is possible to easily determine with very high accuracy which events are bursts, studies should be made on the activity leading up to the burst. Several events have shown periodic indicators of activity before the actual event eruption. However, without in depth study of these and events that do not show such activity, it cannot be determined whether the activity is a precursor, or whether it is unrelated.

### 5.2.4 Tool Enhancement

The Web-based tool developed for remote users could be expanded to provide more types of online data analysis. Presently, the tool allows users to search for events meeting specific criteria, and several reports are available to the user. However, for some analysis, it is still necessary to download these reports and perform additional offline analysis to get some types of reports. Similarly, the user interface could be enhanced so as to be simpler for more people to easily and quickly use.

### 5.2.5 Incorporating Location Information

For the most part, this study has not made use of the burst location ability of SRBL. This is partially due to the fact that SRBL only attempts to find the location of very powerful events. During the present portion of the solar cycle, very few of these events occur. However, as solar activity increases in the next few years, more studies of the results of SRBL's burst locating abilities can be made. This information could be incorporated into overall burst information as well as the Web-based tool.

### 5.3 Conclusion

In conclusion, the research described herein shows that the Solar Radio Burst Locator is capable of accurately detecting many solar microwave events. By studying the data that this instrument provides, it is possible to learn more about the events that have been known on many occasions to disrupt communication systems. The analysis presented reveals many characteristics of various types of events recorded by SRBL. This information can be used to enhance the event classification system so as to provide better nowcasts and warnings of solar-induced electromagnetic interference.

## REFERENCES

- [1] Bai, T., Sturrock, P.A., "Classification of Solar Flare," Center for Space Science and Astrophysics, Stanford University, Annual Review of Astro Astrophysics. 1989.
  
- [2] Britt, R. R., "Powerful Solar Storm to Hit Earth by Wednesday", Space.com, [http://www.space.com/scienceastronomy/solar\\_storm\\_050118.html](http://www.space.com/scienceastronomy/solar_storm_050118.html), Jan. 18, 2005.
  
- [3] Buonsanto, M.J., Fuller-Rowell, T.J., "Strides Made in Understanding Space Weather at Earth," Eos Vol. 78, No. 1, American Geophysical Union, pp. 6-7, Jan. 7, 1997.
  
- [4] "Chemical Composition of Stars," Ask an Astrophysicist, Goddard Space Flight Center, [http://imagine.gsfc.nasa.gov/docs/ask\\_astro/answers/961112a.html](http://imagine.gsfc.nasa.gov/docs/ask_astro/answers/961112a.html), Nov. 1996, retrieved Oct. 14, 2006.
  
- [5] Classen, H.T., Aurass, H., "On the association between type II radio bursts and CMEs," Astronomy & Astrophysics, 384, pp. 1098-1106, 2002.

- [6] "Communications and Space Weather," Australian Government IPS, Radio and Space Services, The Australian Space Weather Agency,  
<http://www.ips.gov.au/Educational/1/3/4>
- [7] Dougherty, B.L., "SRBL prototype evaluation 1: A comparison of flux measurements, location results, and timing reports for several simultaneously recorded large microwave bursts from RSTN, SOON, and the SRBL prototype at OVRO." Nov. 2000.
- [8] Dougherty, B.L., "Technical Review of the Solar Radio Burst Locator," California Institute of Technology, July 2001.
- [9] Dougherty, B.L., Freely W.B, and Zirin H. "Solar Radio Burst Location," High Energy Solar Physics: Anticipating HESSI, ASP Conferences Series, Vol. xxx, 2000.
- [10] Dougherty, B.L, Zirin, H., Hsu, K., "Statistical Correlations Between Solar Microwave Bursts and Coronal Mass Ejections," The Astrophysical Journal, American Astronomical Society, 577, pp 457-463, Sept. 2002.
- [11] "Edited Solar Events Lists," National Oceanic & Atmospheric Administration,  
<http://www.sec.noaa.gov/ftpdir/indices/events/README>, June 2006.

- [12] Fayyad, U. M., et. al., Advances in Knowledge Discovery & Data Mining, American Association for Artificial Intelligence, 1996.
- [13] Hwangbo, J.-E., et. al., "An Evaluation of the Solar Radio Burst Locator (SRBL) at OVRO," *Journal of Korean Astronomical Society*, 38, pp, 437-443, 2005.
- [14] "Internet Space Weather and Radio Propagation Forecasting Course," *Solar Terrestrial Dispatch*, 2001.
- [15] Kantardzic, M., Data Mining: Concepts, Models, Methods, and Algorithms, IEEE Press, 2001.
- [16] Kiplinger A., "Use of the Solar Radio Burst Locator Telescopes", 2002 CIPS Annual Report, Center for Integrated Plasma Studies, University of Colorado at Boulder, CO, USA, pp. 43, Aug. 2003.
- [17] Koons, H.C., et. al., "The Impact of the Space Environment on Space Systems", 6th Spacecraft Charging Technology Conference, AFRL-VS-TR-20001578, pp. 7-11, Sept. 1, 2000.
- [18] Newsom, H.E., "Composition of the Solar System, Planets, Meteorites, and Major Terrestrial Reservoirs," *Global Earth Physics: A Handbook of Physical Constants*, American Geophysical Union, pp. 159-189.

- [19] "Solar Radio Flux Data Lists," National Oceanic & Atmospheric Administration, <http://sec.noaa.gov/ftpdir/lists/radio/README>, August 2006.
- [20] SRBL Operator and Training Course
- [21] Technical Manuel – Maintenance. T.O. SRBL-MM-20021105 For the Solar Radio Burst Locator (SRBL) A/F24U-9. Raytheon Technical Services Company. Dec. 2002.
- [22] Witten, I. A., Frank, E., Data Mining: Practical Machine Learning Tools and Techniques with Java Implementations. Morgan Kaufmann Publishers, 2000.